1-1-2008

Analysis of stacked retaining walls

Layne David Weight
University of Nevada, Las Vegas

ANALYSIS OF STACKED RETAINING WALLS

by

Layne David Weight

Bachelor of Science in Engineering, Civil Engineering
University of Nevada, Las Vegas
2003

A thesis submitted in partial fulfillment
of the requirements for the

Master of Science Degree in Engineering
Department of Civil and Environmental Engineering
Howard R. Hughes College of Engineering

Graduate College
University of Nevada, Las Vegas
May 2008

UNLV
UNIVERSITY OF NEVADA LAS VEGAS

Thesis Approval
The Graduate College
University of Nevada, Las Vegas

April 25, 2008

The Thesis prepared by

Layne David Weight

Entitled

Analysis of Stacked Retaining Walls

is approved in partial fulfillment of the requirements for the degree of

Master of Science Degree in Engineering

Examination Committee Chair

Dean of the Graduate College

Examination Committee Member

Examination Committee Member

Graduate College Faculty Representative

1017-53

ABSTRACT

Analysis of Stacked Retaining Walls

by

Layne David Weight

Moses Karakouzian, Ph.D.
Professor of Civil Engineering
University of Nevada, Las Vegas

Not much literature is available which addresses the analysis of stacked retaining walls. Many designers have developed undocumented and informal methods of analysis based on geotechnical theory, practical experience and intuition.

This thesis presents and compares results from eight common methods of analysis: four methods based on limit equilibrium, three based on elastic theory, and one that is a combination of limit equilibrium and elastic theory. These eight different methods were used to analyze 64 different configurations of double-stacked cantilever retaining walls, including a double-stacked configuration that failed in 1992. In all, results from a total of 512 separate analyses are presented and compared herein, including analysis with a finite element computer application, Plaxis.

The results of these analyses follow the generally accepted notion that as the horizontal spacing between double-stacked walls decreases, the forces at the lower wall increase due to the effects of the upper wall. No method of analysis consistently yields the most or least conservative values, suggesting that the retaining wall designer need take great care in selecting a method of analysis.

TABLE OF CONTENTS

ABSTRACT iii

LIST OF FIGURES vi

LIST OF TABLES viii

CHAPTER 1 INTRODUCTION
1.1 Background 1
1.2 Motivation 5
1.3 Previous Work 6
1.4 Objective 6

CHAPTER 2 METHODOLOGY
2.1 STEP 1 Design Stacked Configurations 9
2.2 STEP 2 Identify Methods of Analysis 10
2.3 STEP 3 Analysis of Stacked Configurations 11
2.4 STEP 4 Results 11
2.4 STEP 5 Conclusions and Recommendations 12

CHAPTER 3 DESIGN OF STACKED CONFIGURATIONS
3.1 Geometry of Stacked Configurations 13
3.2 Material Properties 14
3.3 Design of Retaining Walls 16

CHAPTER 4 IDENTIFY METHODS OF ANALYSIS
4.1 Commonly Used Methods of Analysis 24
4.1.1 Analysis Based on Limit Equilibrium 24
4.1.1.1 Equivalent Backfill Slope 25
4.1.1.2 Uniform Surcharge 26
4.1.1.3 Culmann's Graphical 27
4.1.1.4 Method of Slices 28
4.1.1.5 Olson 30
4.1.2 Analysis Based on Elastic Theory 31
4.1.2.1 Boussinesq and Others 31
4.1.2.2 Numerical Analysis 35
4.1.3 Analysis Based on Limit Equilibrium and Elastic Theory 37
4.2 Methods of Analysis Selected for Thesis Study 39

CHAPTER 5 ANALYSIS OF STACKED CONFIGURATIONS
5.1 Example Analyses and Results for Methods Selected for Thesis Study 40

5.1.1 Method 1 Equivalent Backfill Slope (Rankine) 40
5.1.2 Method 2 Equivalent Backfill Slope (Coulomb) 42
5.1.3 Method 3 Uniform Surcharge 43
5.1.4 Method 4 Culmann's Graphical 45
5.1.5 Method 5 Elastic Theory (Jarquio) 54
5.1.6 Method 6 Elastic Theory (Terzaghi) 55
5.1.7 Method 7 Numerical Analysis / Finite Element (Plaxis) 56
5.1.8 Method 8 Brooks Surcharge 62
5.2 Analysis of a Post-Failure Case Study 65

CHAPTER 6 RESULTS
6.1 Results for Thesis Study 67
6.2 Results for Post-Failure Case Study 78

CHAPTER 7 CONCLUSIONS AND RECOMMENDATIONS
7.1 Conclusions 81
7.1.1 Overall 81
7.1.2 Method Specific 83
7.1.2.1 Equivalent Backfill Slope 84
7.1.2.2 Uniform Surcharge 85
7.1.2.3 Culmann's Graphical 85
7.1.2.4 Elastic Theory 87
7.1.2.5 Finite Element 87
7.1.2.6 Brooks 87
7.2 Recommendations 88

REFERENCES 91

APPENDIX A SYSTEMS RESISTING SLIDING AND OVERTURNING 93

APPENDIX B CALCULATIONS FOR METHODS EBS, US, CG, FEA-P AND BS... 96

APPENDIX C CALCULATIONS FOR METHODS ET 103

APPENDIX D SECTION PROPERTIES FOR INPUT INTO PLAXIS 172

APPENDIX E LATERAL PRESSURE OUTPUT FROM PLAXIS 186

APPENDIX F TABLES OF RESULTS 250

APPENDIX G CHARTS 255

VITA 302

LIST OF FIGURES

Figure 1.1 Section at slope between two structures 2
Figure 1.2 Section at retaining wall between two structures 2
Figure 1.3 Section at stacked retaining walls 3
Figure 1.4 Photograph of a four level group of stacked retaining walls 3
Figure 1.5 Photograph of a four level group of stacked retaining walls 4
Figure 1.6 Photograph of a five level group of stacked retaining walls 4
Figure 3.1 Key for Table 3.1, geometry of stacked retaining walls 14
Figure 3.2 Double-stacked configuration of failure case study 14
Figure 3.3 Key for Table 3.3, design of individual retaining walls 16
Figure 3.4 Overturning analysis at upper retaining walls 18
Figure 3.5 Overturning analysis at lower retaining walls 19
Figure 3.6 Key for Table 3.6 20
Figure 4.1 Equivalent Backfill Slope Method 26
Figure 4.2 Uniform Surcharge Method 27
Figure 4.3 Schematic of Culmann's Graphical Method 28
Figure 4.4 Method of Slices 30
Figure 4.5 Olson Method 31
Figure 4.6 Elastic Theory Method 32
Figure 4.7 Boussinesq Elastic Theory 34
Figure 4.8 Terzaghi Elastic Theory 34
Figure 4.9 Jarquio Elastic Theory 35
Figure 4.10 Brooks Surcharge Method 39
Figure 5.1 Equivalent Backfill Slope Method at 5-5-5 configuration 41
Figure 5.2 Uniform Surcharge Method at 5-5-5 configuration 45
Figure 5.3 Culmann's Graphical Method Steps 1 and 2 48
Figure 5.4 Culmann's Graphical Method Steps 3 and 4 49
Figure 5.5 Culmann's Graphical Method Step 5 50
Figure 5.6 Culmann's Graphical Method Steps 7 and 8 51
Figure 5.7 Culmann's Graphical Method Steps 9 and 10 52
Figure 5.8 Culmann's Graphical Method Step 11 52
Figure 5.9 Culmann's Graphical Method Step 12 53
Figure 5.10 Backfill lifts for Plaxis 58
Figure 5.11 Overall geometry proportions used in the Plaxis models. 59
Figure 5.12 Output window of 5-5-5 model in Plaxis 61
Figure 5.13 Output at section A-A* at 5-5-5 model in Plaxis 62
Figure 6.1 Sliding force with respect to C at A=B=5 configuration 68
Figure 6.2 Overturning moment with respect to C at A=B=5 configuration 69
Figure 6.3 Factor of safety against sliding with respect C at A=B=5 69
Figure 6.4 Factor of safety against overturning with respect C at A=B=5 70
Figure 6.5 Sliding force with respect to C all configurations 74

Figure 6.6 Overturning moment with respect to C at all configurations 75
Figure 6.7 Factor of safety against sliding with respect C at all config............................ 76
Figure 6.8 Factor of safety against overturning with respect C at all config.................... 77
Figure 6.9 Photograph of double-stacked failure.. 80

LIST OF TABLES

Table 3.1 Geometry of stacked retaining walls shown in Figure 3.1 14
Table 3.2 Soil properties for failure case study 15
Table 3.3 Design of individual stacked retaining walls shown in Figure 3.3 17
Table 3.4 Results of overturning and bearing analyses at upper retaining walls.............. 18
Table 3.5 Legend for marks used in tables 3.6 and 3.7 21
Table 3.6 Results of internal stability design of retaining walls...................................... 21
Table 3.7 Material properties for retaining wall panels and footings input into Plaxis.... 23
Table 4.1 Legend for Mark at Methods of Analysis... 39
Table 5.1 Soil material properties input into Plaxis for post-failure case study 66
Table 6.1 Sliding force and overturning moment at 5-15-20 configuration..................... 71
Table 6.2 Sliding force count.. 72
Table 6.3 Overturning moment count... 72
Table 6.4 Factor of safety against sliding count 72
Table 6.5 Factor of safety against overturning count 73
Table 6.6 Results of failure case study 79

CHAPTER 1

INTRODUCTION

1.1 Background

Retaining walls are currently popular with residential and commercial developers in the Las Vegas, Nevada, area. When compared to the use of a conventional cut or fill slope, the use of a retaining wall generally results in more developable land, as shown in Figures 1.1 and 1.2. The term "stacked retaining walls", as shown in Figure 1.3, is used to describe a group of retaining walls that are constructed at different elevations and set back horizontally with respect to each other to create a "terraced" appearance. The use of stacked retaining walls are often preferred over the use of one large retaining wall as they can often result in a cost savings are generally considered a more aesthetically pleasing alternate to the use of just one retaining wall. For this reason, stacked retaining walls are commonly selected at hilly commercial and residential sites. Stacked retaining walls are a common site in many of the residential developments of the Las Vegas, Nevada, area. Figures 1.4 through 1.6 are photographs of retaining walls arranged in stacked configurations located at various residential developments in the Las Vegas, Nevada, area.

In addition to the term "stacked retaining walls", other terms that are commonly used are "terraced retaining walls", "multi-tier retaining walls", "multiple level retaining walls", "cascading retaining walls", "piggyback retaining walls" and "benched retaining walls". The term "lower stacked retaining walls" as it appears herein refers to the lower wall(s) in a stacked configuration.

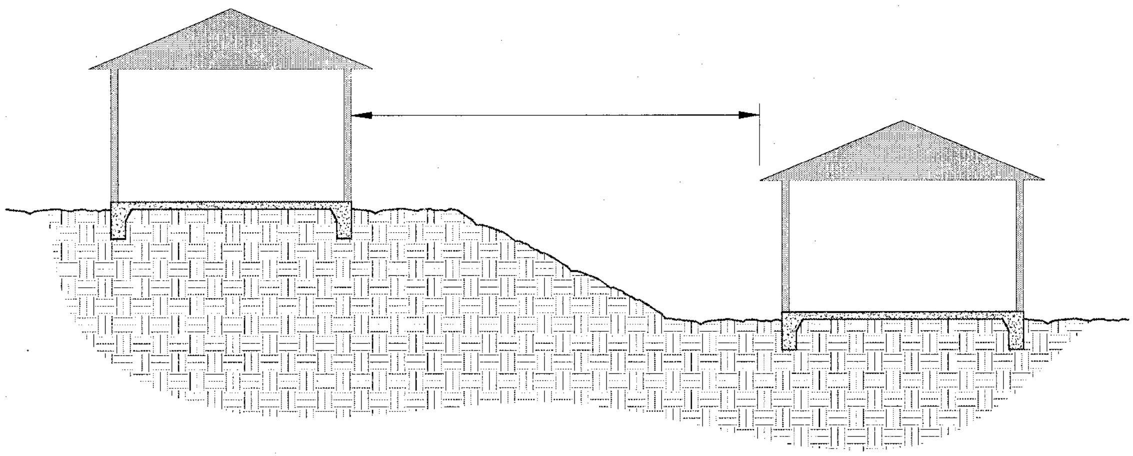

Figure 1.1. Section showing the a slope between two structures that are at different elevations with respect to each other.

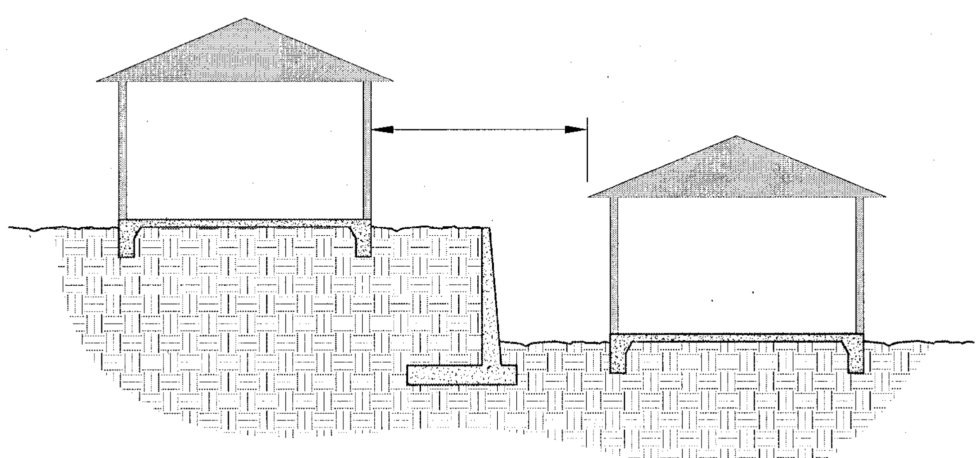

Figure 1.2. Section showing the use of a cantilever retaining wall between two structures rather than a slope (Figure 1.1) to allow the structures, such as those of a residential tract development, to be spaced closer together resulting in more developable land.

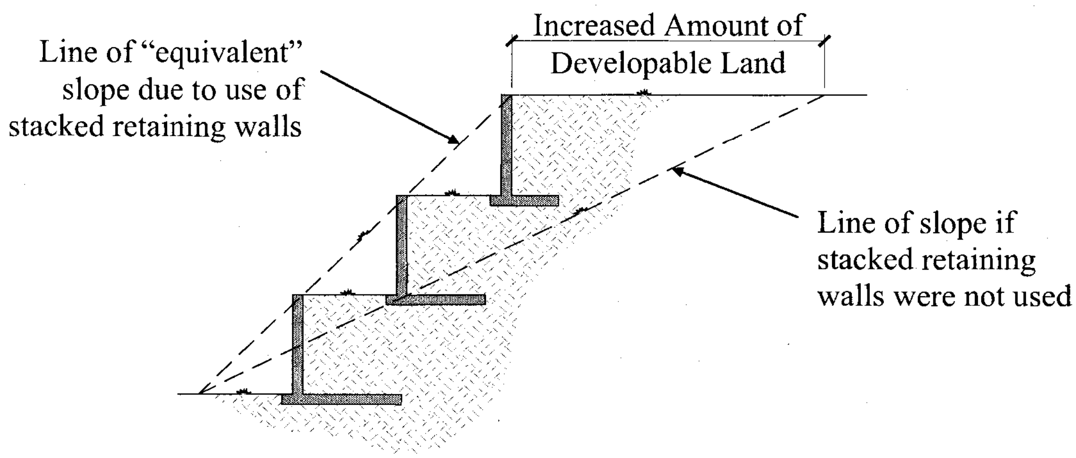

Figure 1.3. Section showing the use of stacked cantilever retaining walls to increase the amount of developable land compared to a cut / fill slope.

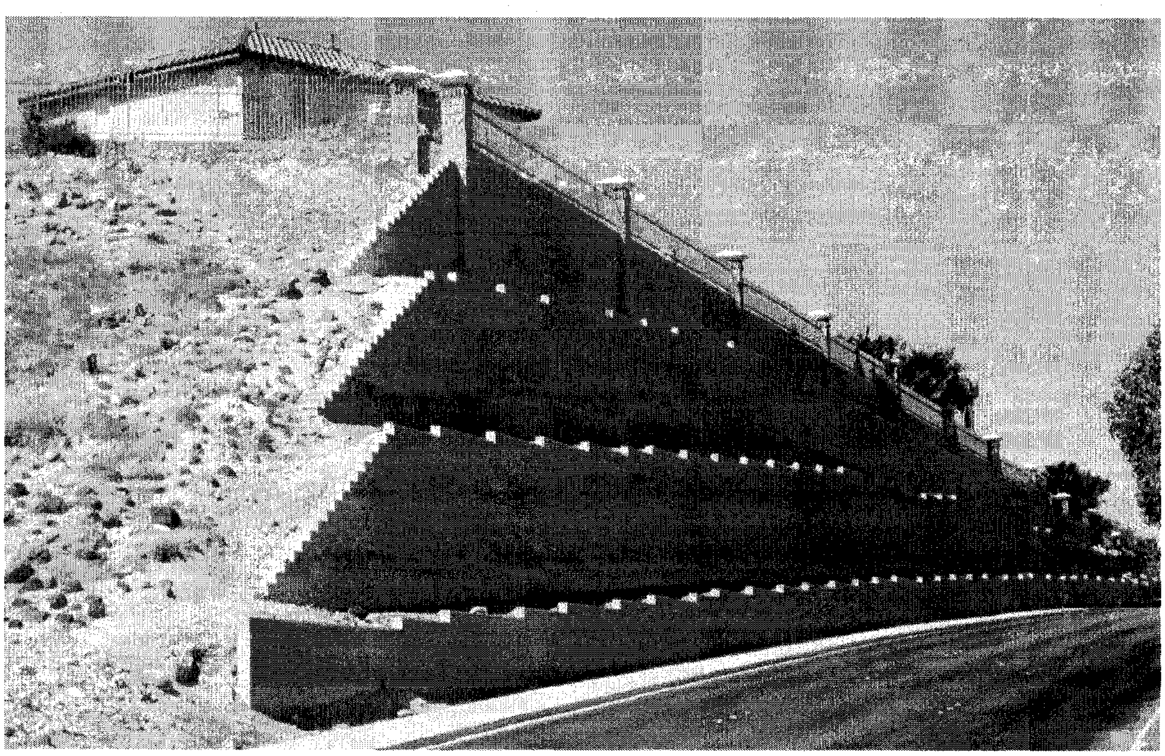

Figure 1.4. Four reinforced concrete / masonry cantilever retaining walls constructed in a "stacked" configuration located along Sunridge Heights Parkway east of Seven Hills Drive.

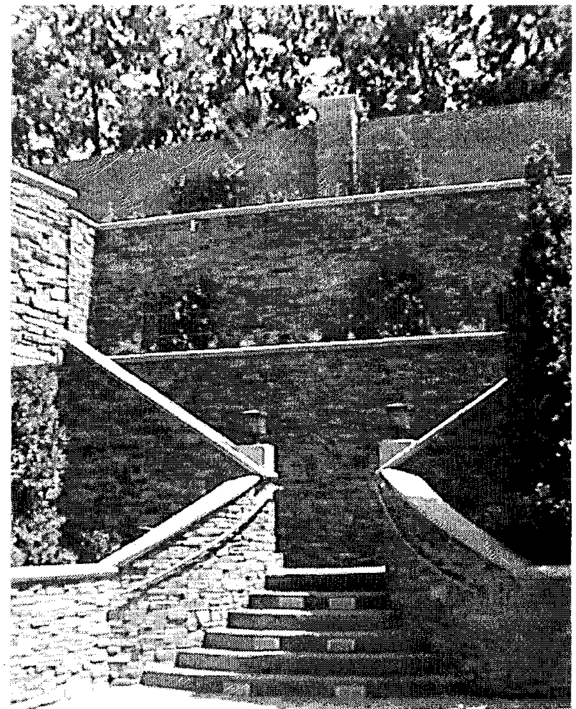

Figure 1.5. Four reinforced concrete cantilever retaining walls constructed in a "stacked" configuration at the site of a custom residence.

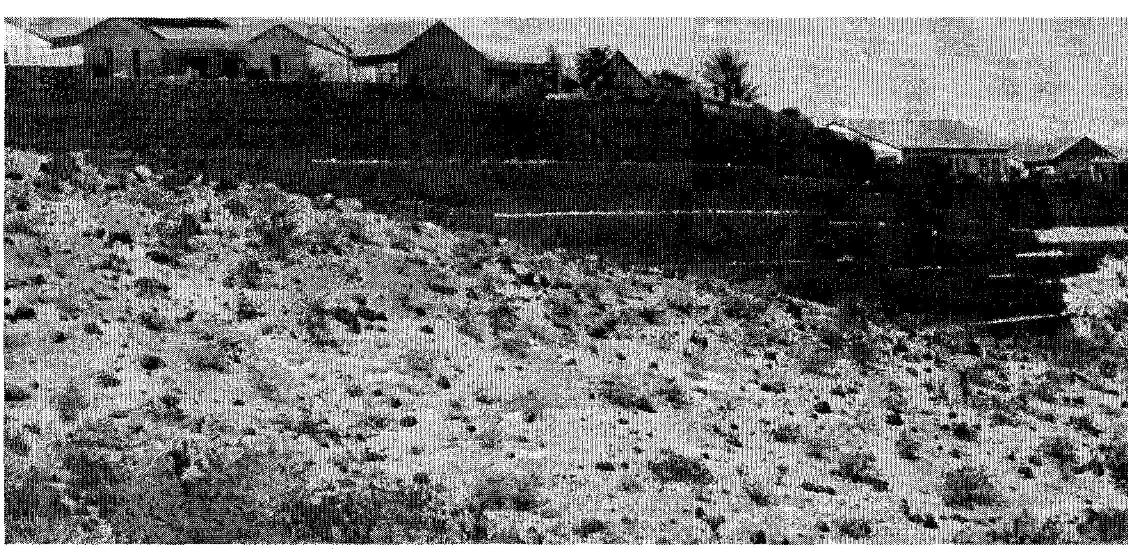

Figure 1.6. Five reinforced concrete / masonry cantilever retaining walls constructed in a "stacked" configuration used at the edge of a residential development to create more developable land.

1.2 Motivation

The analysis of the lower retaining walls of a stacked configuration presents a special challenge to the civil engineer: what are the additional horizontal earth pressures at the lower retaining walls due to the effects of the upper retaining walls? There are no established methods of analysis nor is there much literature is available to the retaining wall designer regarding methods of analysis to determine the horizontal pressures at lower stacked retaining walls.

Due to the popularity of stacked retaining walls, designers have developed many different undocumented and informal methods of analysis based on geotechnical theory, practical experience and intuition. However, as will be demonstrated herein, the use of one method may require that a lower retaining wall of a double-stacked configuration be designed for two, five, or even ten times as much flexural, sliding and/or overturning force than a different method of analysis might require. With such a wide range of results for a stacked configuration, it is difficult for the designer to know which method is safe to select. Is one method of analysis generally the most conservative? Is another method of analysis generally the least conservative? Is one method of analysis better suited for a particular stacked configuration than another? Has any testing been done to validate any of the methods of analysis?

The objective of the typical retaining wall engineer is to provide their client with a design that will not only be stable against the forces to which the retaining wall may be subjected, but will not be so overly conservative as to cost an unreasonable amount to construct. If the designer selects what appears to be the least conservative method of analysis for a particular stacked configuration, will the resulting design be adequate?

1.3 Previous Work

Surprisingly, the topic of analysis of stacked retaining walls does not appear to have been studied seriously, even though stacked configurations of retaining walls are frequently constructed. In fact, during the literature review for this thesis, only three published works were found which specifically address the topic of analysis of stacked retaining walls[1, 2, 3]. Each of these works presents a different method of analysis. One of these published works[1] recommends that stacked retaining walls be analyzed for lateral earth pressure based on a elastic theory equation[4] developed in the 1930s in response to the results of full-scale experiments. However, it should be noted that the experiments performed in the 1930s did not specifically address stacked configurations of retaining walls, but rather backfill surface loads at cantilever retaining walls. Another work encountered during literature review is a self-published retaining wall guide[2] and proposes two separate methods of analysis based on limit equilibrium and elastic theory. Another published work[3] presents a post-failure analysis of a double-stacked configuration that utilizes a computer application to analyze the lower wall. The computer application analysis is based on limit equilibrium and was developed by the author of the work specifically for the post-failure analysis. More specific information regarding the methods of analysis presented in the three published works mentioned above is provided in Chapter 4 of this thesis.

1.4 Objectives

The analysis of stacked retaining walls is complex. The scope of this thesis does not attempt to be all-inclusive. This thesis presents a modest collection of commonly used methods of analysis for stacked retaining walls, many of them undocumented and informal, and then compares results of these methods applied to the analysis of the lower wall of a double-stacked configuration of cantilever retaining walls. The primary objective of the work presented herein is not to present every method of analysis currently used by retaining wall engineers, nor to propose a new method of analysis. The primary objective of this thesis is quite simply to attempt to show that more detailed research on this topic is desperately needed.

The ideal research, of course, would be to use extant methods of analysis to predict earth pressures and wall and footing stresses and displacements at retaining walls of different stacked configurations, construct and instrument these configurations of stacked retaining walls, and either validate a particular method of analysis, or develop entirely new methods of analysis. However, since this type of research is probably very costly and will require a great deal of effort and time to complete, it is likely that results from any such research will not be available for some time. What does the retaining wall design community do in the interim? The secondary objective of the work presented herein is to attempt to provide the retaining wall design community with some general guidelines for the selection of a method of analysis while the retaining wall design community waits for results of more detailed research. Since most of the methods of analysis currently in use by the retaining wall engineers of the world are probably undocumented and informal methods, the collection of analysis methods presented in this thesis could not possibly represent all of the methods currently in use. However, perhaps a retaining wall designer somewhere in the world that has developed their own method of analysis possibly different from those presented in this thesis could use the information presented herein to measure their method of analysis and, as needed, adjust and refine their method.

CHAPTER 2

METHODOLOGY

2.1 STEP 1 Design of Stacked Configurations

The results from several different methods of analysis of stacked retaining walls are compared in this thesis. Specifically, these methods of analysis are applied to reinforced concrete cantilever retaining walls arranged in pairs of stacked configurations. For the purposes of this thesis, these configurations of retaining walls are referred to as "double-stacked." To explore whether one method of analysis is better suited for a particular double-stacked configuration, the heights and horizontal offsets of stacked retaining walls were varied. In order to accomplish this, six individual cantilever retaining walls of varying heights were paired to create a total of 63 separate configurations of double-stacked cantilever retaining walls.

The results of analysis of cantilever retaining walls depend very much on the length and thickness of the footing and wall panels. In order to ensure that the methods of analysis were compared equally, the geometry and stiffness of each cantilever retaining wall was determined. In other words, each individual retaining wall was designed prior to performing the analysis of the stacked configurations. A total of six different reinforced concrete cantilever retaining walls were designed: three upper walls and three lower walls.

The results of analysis of cantilever retaining walls also depends greatly upon the properties of the backfill and subgrade soil material. For this reason, the soil properties at all 63 double-stacked configurations were maintained constant. To simplify the analyses, the backfill and subgrade material of each retaining wall was assumed to be a homogeneous and drained sandy material and the effects of a water table at the backfill or subgrade was not considered.

As mentioned in section 1.3 above, a double-stacked configuration of retaining walls failed in 1992. A post-failure analysis[3] of these retaining walls provides fairly detailed information regarding the geometry of the stacked configuration, the thickness and length of each wall and footing panel, and the properties of the subgrade and backfill soil material. The report also provides the results of the post-failure analysis of the lower stacked wall. Thus, in addition to the 63 double-stacked configurations of retaining walls described above, the double-stacked configuration of retaining walls that failed in 1992 was also analyzed with the same methods of analysis applied to the 63 configurations.

2.2 STEP 2 Identify Methods of Analysis

The first part of Step 2 was to identify commonly used method of analysis available in either published works or directly from retaining wall engineers. As mentioned in Chapter 1, not much literature is available which specifically addresses the analysis of stacked retaining walls, and many methods of analysis currently used in professional design practice are not documented. Thus, the methods identified in this first part of Step 1 do not attempt to be an all-inclusive listing of every method of analysis available to retaining wall designers.

The second part of Step 2 was to select a few of these methods identified as commonly used to analyze the 64 stacked configurations of cantilever retaining walls described above in Step 1. A few of the methods of analysis selected for this thesis were taken from literature, while others were encountered during the professional retaining wall design experience of the author of this thesis. Finite element software which specializes in geotechnical applications, was also selected as a method to analyze the stacked configurations. In all a total of eight different methods of analysis were selected to analyze each of the 64 stacked configurations.

2.3 STEP 3 Analysis of Stacked Configurations

Once the geometry and material properties were set, and the methods of analysis identified, each of the 64 different configurations of the stacked retaining walls was analyzed using the eight different methods of analysis. In all, a total of 512 separate analyses were performed. An example calculation for just one double-stacked configuration is provided here for each of the eight different methods of analysis, as well as more specific information regarding the analysis with the eight methods applied to the lower wall of the double-stacked configuration that failed in 1992.

2.4 STEP 4 Results

The results of the 504 separate analyses at the first 63 double-stacked configurations of retaining walls are presented and compared to each other with the aid of charts and tables. Also, the results of the analysis with the eight methods applied to the double-stacked configuration that failed in 1992 are presented and then compared to the results of the analysis provided by the author of the post-failure report. In all, results are presented for all 512 analyses described in Step 3.

2.5 STEP 5 Conclusions and Recommendations

Conclusions and recommendations are provided based on an analysis of the results presented in steps 3 and 4. The recommendations also identify potential areas of future work.

CHAPTER 3

DESIGN OF STACKED CONFIGURATIONS

3.1 Geometry of Stacked Configurations

As described in Step 1 above, this thesis compares lateral earth pressures at reinforced concrete cantilever retaining walls arranged in double-stacked configurations. The geometry of 63 of the 64 double-stacked configurations was arbitrarily determined as shown in Figure 3.1, and Table 3.1. The geometry of the 64th double-stacked set of retaining walls was taken from the post-failure report[3] described in Chapter 1 and is presented in Figure 3.2.

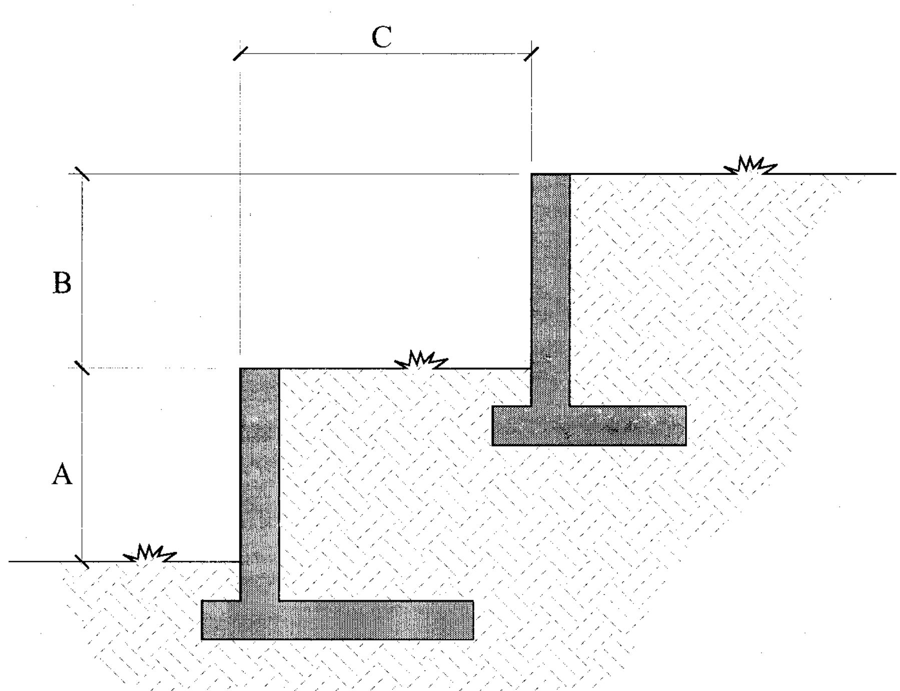

Figure 3.1. Double-stacked configuration used for thesis. Heights, A and B, and horizontal offset, C, at increments shown in Table 3.1 to create 63 different stacked configurations.

Table 3.1. Increments of wall heights and horizontal offsets at dimension mark shown in Figure 3.1.

Mark at Figure 3.1	Increments of Height / Horizontal Offset
A	5 ft, 10 ft, 15 ft
B	5 ft, 10 ft, 15 ft
C	5 ft, 7.5 ft, 10 ft, 12.5 ft, 15 ft, 17.5 ft, 20 ft

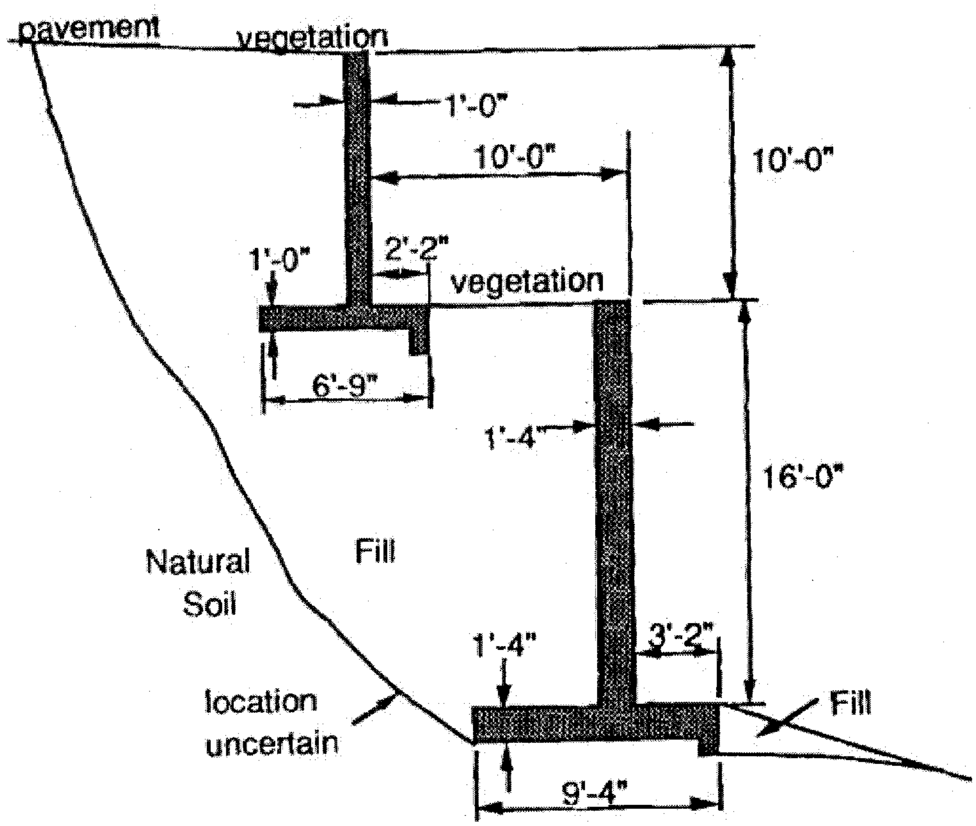

Figure 3.2. Configuration of double-stacked retaining walls that failed in 1992 (taken from Olson[3]).

3.2 Material Properties

As described above, the soil parameters were held constant for all analyses, and a homogeneous and drained sandy material was selected. The principal properties of this sandy material are a unit weight, γ, of 110 pcf (pounds per cubic foot), an internal angle of friction, ϕ, of 34 degrees, and soil cohesion, c, of zero psf (pounds per square foot).

As mentioned above, one of the eight methods of analysis employs the use of a finite element software called Plaxis. Plaxis requires that additional information be input regarding the properties of the soil. The material properties input into Plaxis for the soil are presented in Table 3.2. Although the subgrade and backfill material are assumed to be a cohesionless sand, it should be noted that Plaxis requires at least some amount of cohesion in order to "improve calculation performance." Thus, a negligible value is used for the soil cohesion, c.

Table 3.2. Soil material properties input into Plaxis.

Material Property	Description	Value
γ_{unsat}	Unsaturated Unit Weight of Soil	110 pcf
k_x	Permeability in the x direction	3 ft / day
k_y	Permeability in the y direction	3 ft / day
E	Young's Modulus	1,000,000 psf
ν	Poisson's Ratio	0.3
c	Soil Cohesion	0.05 psf
ϕ	Angle of Internal Friction	34°

As described below in section 3.3 of this chapter, each individual retaining wall was designed prior to commencing the analysis phase. In order to design the retaining walls, the properties of the concrete and reinforcing steel were established. The retaining wall designs were based on a concrete assumed to be normal weight with a unit weight of 150 pcf, and a 28-day compressive strength, f'_c, of 2,500 psi (pounds per square inch), and the reinforcing steel was assumed to have a yield strength, f_y, of 60,000 psi.

3.3 Design of Retaining Walls

Since the analysis of a cantilever retaining wall depends upon the width and thickness of each wall and footing panel as described in Chapter 2, each individual cantilever retaining wall was designed prior to beginning analysis. These designs, based on the professional experience of the author of this thesis and not any particular method of analysis, are presented in Figure 3.3 and Table 3.3.

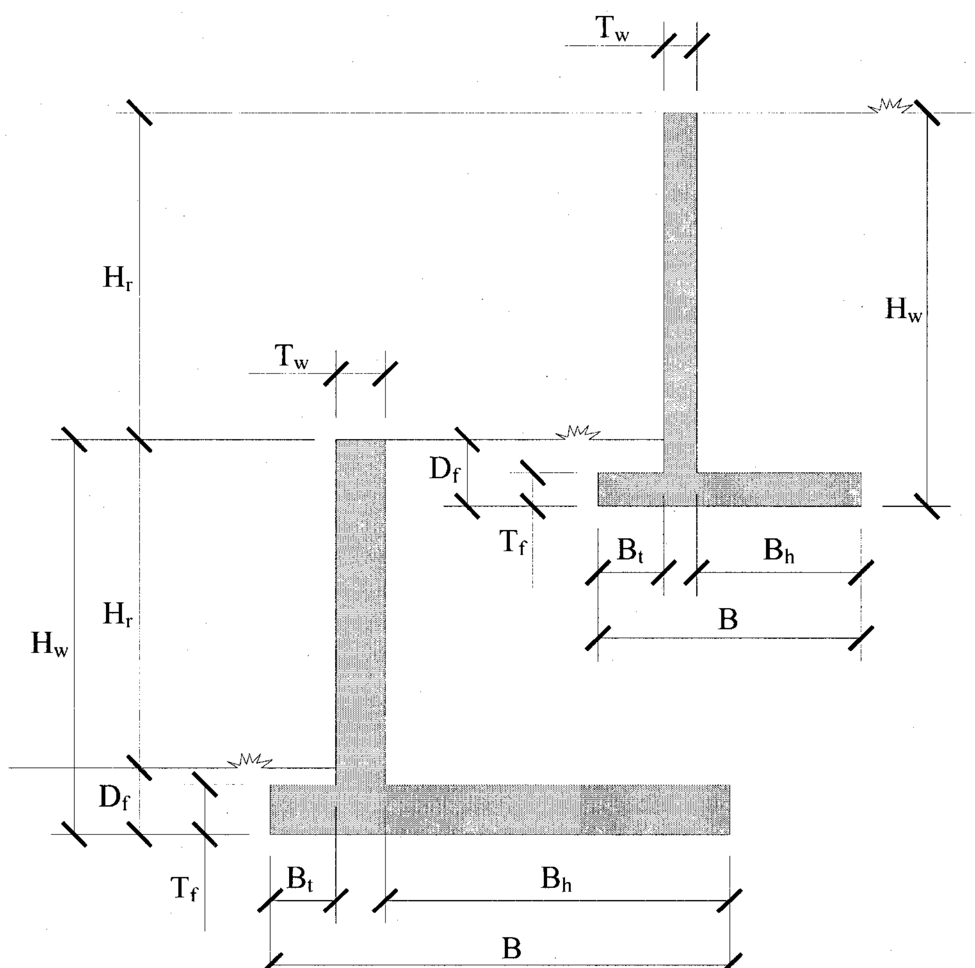

Figure 3.3. Legend for Table 3.3 for design of upper and lower stacked retaining walls.

Table 3.3. Designs of upper and lower walls (see Figure 3.3).

	Lower Walls			Upper Walls		
H_w	7 ft	12 ft	17 ft	7 ft	12 ft	17 ft
H_r	5 ft	10 ft	15 ft	5 ft	10 ft	15 ft
D_f	2 ft	2 ft	2 ft	2 ft	2 ft	2 ft
T_f, T_w	1 ft	1.5 ft	2 ft	1 ft	1 ft	1.5 ft
B	7 ft	14 ft	20 ft	5 ft	8 ft	10 ft
B_t	1 ft	2 ft	3 ft	1 ft	2 ft	2 ft
B_h	5 ft	10.5 ft	15 ft	3 ft	5 ft	6.5 ft

Three of the eight methods of analysis selected require that the resultant bearing pressure distribution at the upper wall be determined. In order to complete a bearing pressure analysis, the overturning moments of the upper wall needed to be determined according to traditional eccentric bearing pressure analysis presented on page 402 of Das[10]. The overturning moment was determined per traditional Rankine active earth pressure theory. The coefficient of active earth pressure, K_a, according to Rankine theory is equal to $TAN^2 (45° - \phi / 2)$ for level backfill slope. For ϕ equal to 34°, K_a is 0.283 and the equivalent fluid active unit weight of the backfill material is equal to γ times K_a, or 31 pcf. The moment resisting overturning was calculated based on the traditional methods of calculating the weight of the wall and footing, the weight of the soil over the footing as shown in Figure 3.4. The passive pressure at the toe of the upper retaining wall was included in the overturning moment. This pressure was calculated based on Rankine theory. The coefficient of passive earth pressure, K_p, according to Rankine theory is equal to $TAN^2 (45° + \phi / 2)$ for level slope at the toe. For ϕ equal to 34°, K_p is 3.54. The equivalent fluid passive unit weight of the backfill material is equal to γ times K_p, or 389 pcf. The overturning moments and bearing pressure distributions calculated at the three upper walls is displayed in Table 3.4.

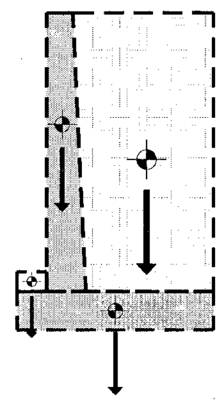

Figure 3.4. Areas used to calculate weight per foot of length of the wall, footing, and soil over the toe and heel of the upper retaining wall for overturning and bearing pressures analysis.

Table 3.4. Overturning and resisting moments, and bearing pressure distribution at upper retaining walls of stacked configurations. Refer to Figure 3.3 for H_r.

H_r	$M_{overturn}$	$M_{total\ resist}$	q_{toe}	q_{heel}
5 ft	1,778 ft-lb	10,730 ft-lb	844 psf	652 psf
10 ft	8,956 ft-lb	42,940 ft-lb	1,374 psf	906 psf
15 ft	25,465 ft-lb	96,274 ft-lb	2,523 psf	863 psf

The system resisting sliding and overturning at the lower wall was also calculated according to traditional retaining wall design available in any geotechnical textbook. For these calculations, the weight of the upper wall and soil at the upper wall was considered as shown in Figure 3.5. This weight was determined for the lower wall of each of the 64 different configurations of stacked retaining walls and is presented in Appendix A.

The coefficient of friction, μ, at the bottom of the concrete footing to the soil and, for the purposes of Coulomb theory, at the soil face of the wall panel, was determined to calculate the force resisting system sliding. The coefficient of friction is TAN (0.67 ϕ). For ϕ equal to 34°, μ is 0.418. See Appendix A for the system moments resisting overturning and forces resisting sliding at the lower walls of each of the 64 different configurations.

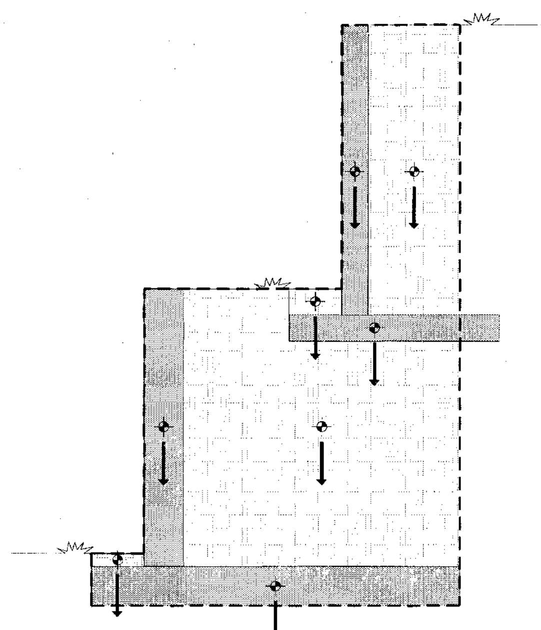

Figure 3.5. Areas used to calculate weight per foot of length of the lower retaining wall for system resisting overturning and sliding analysis.

As mentioned above, one of the eight methods of analysis employs the use of a finite element software called Plaxis. Plaxis requires that information be input regarding the elastic properties of the reinforced concrete retaining wall and footing such as axial stiffness, EA, flexural rigidity, EI, and Poisson's ratio, ν., in addition to physical properties such as weight per foot of length, w. Plaxis also requires information be input regarding elastic properties of the soil such as Young's Modulus, E_{ref}, and Poisson's ratio, ν, in addition to standard soil properties such as the unit weight of the soil, γ, the angle of internal friction, ϕ, the soil cohesion, c.

In order to provide the retaining wall and footing properties required by Plaxis, the walls had to be designed for internal stability, i.e. flexural and shear forces. This design was provided based on the professional experience of the author of this thesis in a manner similar to the design provided for external stability as presented in Figure 3.3 and Table 3.3. The resulting design for internal stability is summarized in Figure 3.6 and Table 3.6. Table 3.5 is provided as a legend for the marks used in Tables 3.6 and 3.7.

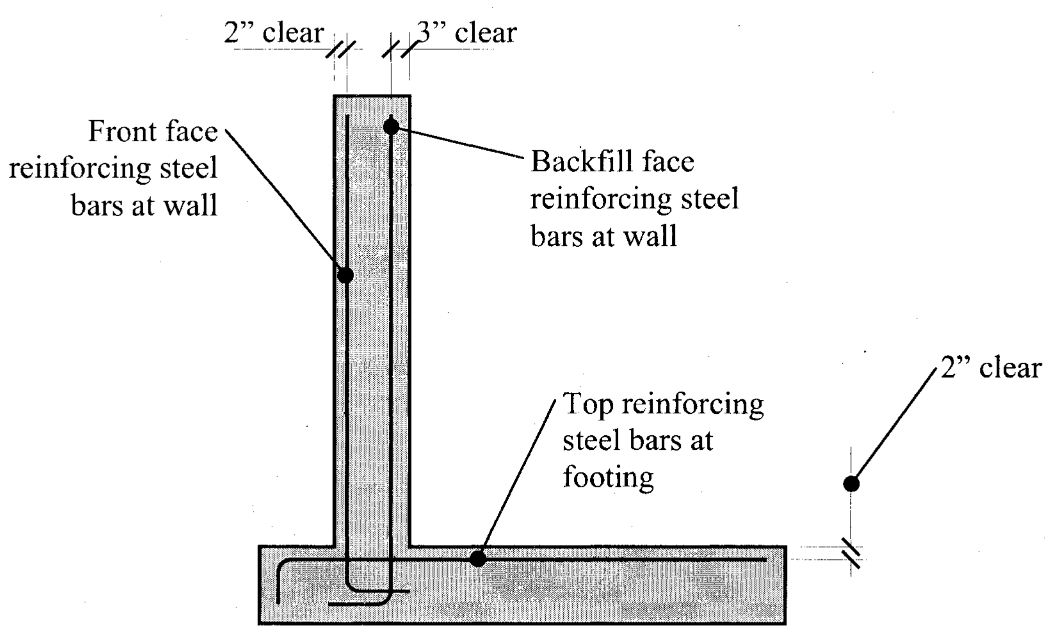

Figure 3.6. Key for Table 3.6, design of reinforced concrete wall and footing panels for internal stability.

Table 3.5. Legend for Marks used in Tables 3.6 and 3.7. See Figure 3.3 and Table 3.3 for information regarding H_w.

Mark	H_w	Upper or Lower wall of Double-Stacked Configuration	Reference to Footing and / or Wall Panel
5U	5 ft	Upper	Footing + Wall
5L	5 ft	Lower	Footing + Wall
10U	10 ft	Upper	Footing + Wall
10L	10 ft	Lower	Footing + Wall
15U	15 ft	Upper	Footing + Wall
15L	15 ft	Lower	Footing + Wall
5UF	5 ft	Upper	Footing Only
5UW	5 ft	Upper	Wall Only
5LF	5 ft	Lower	Footing Only
5LW	5 ft	Lower	Wall Only
10UF	10 ft	Upper	Footing Only
10UW	10 ft	Upper	Wall Only
10LF	10 ft	Lower	Footing Only
10LW	10 ft	Lower	Wall Only
15UF	15 ft	Upper	Footing Only
15UW	15 ft	Upper	Wall Only
15LF	15 ft	Lower	Footing Only
15LW	15 ft	Lower	Wall Only

Table 3.6. Results of internal stability design of retaining walls.

Mark	Backfill Face Bars	Front Face Bars	Top Bars
5U	# 4 at 18 in. o.c.	# 4 at 18 in. o.c.	# 4 at 18 in. o.c.
5L	# 5 at 10 in. o.c.	# 4 at 18 in. o.c.	# 5 at 10 in. o.c.
10U	# 5 at 12 in. o.c.	# 4 at 18 in. o.c.	# 5 at 12 in. o.c.
10L	# 7 at 9 in. o.c.	# 4 at 14 in. o.c.	# 7 at 9 in. o.c.
15U	# 7 at 12 in. o.c.	# 5 at 18 in. o.c.	# 7 at 12 in. o.c.
15L	# 9 at 8 in. o.c.	# 5 at 18 in. o.c.	# 9 at 8 in. o.c.

The material properties for the reinforced concrete footing and wall panels were calculated based on the following equations for a doubly reinforced concrete beam:

$\eta = E_s / E_c$ Equation 3.3.1

$E_c = 57{,}000\ (f'_c)^{0.5}$ Equation 3.3.2

$b\ x^2 / 2 + (\eta-1)\ A'_s\ (x - d') = \eta\ A_s\ (d - x)$ Equation 3.3.3

$I_{cr} = 1/3\ b\ x^3 + (\eta - 1)\ A'_s\ (x - d')^2 + \eta\ A_s\ (d - x)^2$ Equation 3.3.4

$A_c = b\ h$ Equation 3.3.5

$w = \gamma_c\ b$ Equation 3.3.6

Where: η is the ratio of Young's modulus of steel to concrete

E_c is the Young's modulus for concrete (psi)

E_s is the Young's modulus for the reinforcing steel (29,000,000 psi)

f'_c is the 28 day allowable compressive strength of the concrete (2500 psi)

b is the thickness of the wall or footing panel (see Table 3.2)

x is the depth to the neutral axis from the extreme compression fiber (in.)

A'_s is the area of compressive reinforcing steel (in^2)

d' is the depth to the centroid of A'_s from the extreme compression fiber (in)

A_s area of tensile reinforcing steel (in^2)

d is the depth to the centroid of A_s from the extreme compression fiber (in)

I_{cr} is the moment of inertia of the transformed cracked section (in^4)

A_c is the gross area of the cross section (in^2)

h is the width of the section taken as 12" since analysis is per foot of length

w is the weight per foot of length of the section (plf)

γ_c is the unit weight of concrete (150 pcf)

The resulting material properties required for input into Plaxis, E_cA_c, E_c,I_{cr}, b, and w, as defined above are presented in Table 3.7. In addition to the properties presented in Table 3.7, Plaxis also requires a value for Poisson's ratio, ν, for the wall and footing panels. A value of 0.19 is common and was input into the Plaxis finite element model.

Table 3.7. Material properties for reinforced concrete retaining wall panels and footings.

Mark	E_cA_c	E_cI_{cr}	b	w
5UW	410,400,000 lb / ft	1,637,047 lb-ft^2 / ft	1.0 ft	40 lb / ft
5UF	410,400,000 lb / ft	1,637,017 lb- ft^2 / ft	1.0 ft	40 lb / ft
5LW	410,400,000 lb / ft	3,962,534 lb- ft^2 / ft	1.0 ft	40 lb / ft
5LF	410,400,000 lb / ft	3,948,393 lb- ft^2 / ft	1.0 ft	40 lb / ft
10UW	410,400,000 lb / ft	3,398,357 lb- ft^2 / ft	1.0 ft	40 lb / ft
10UF	410,400,000 lb / ft	3,389,295 lb- ft^2 / ft	1.0 ft	40 lb / ft
10LW	615,600,000 lb / ft	23,242,800 lb-f ft^2 / ft	1.5 ft	60 lb / ft
10LF	615,600,000 lb / ft	23,046,333 lb- ft^2 / ft	1.5 ft	60 lb / ft
15UW	615,600,000 lb / ft	18,352,423 lb- ft^2 / ft	1.5 ft	60 lb / ft
15UF	615,600,000 lb / ft	18,200,230 lb- ft^2 / ft	1.5 ft	60 lb / ft
15LW	820,800,000 lb / ft	80,498,842 lb- ft^2 / ft	2.0 ft	80 lb / ft
15LF	820,800,000 lb / ft	79,688,005 lb- ft^2 / ft	2.0 ft	80 lb / ft

The calculations for section properties for input into Plaxis for all eight retaining wall and footing panels are presented in Appendix D.

The report of the retaining walls that failed in 1992 does not provide specific information for the reinforcing and concrete used. As such, the properties for 10UW, 10UF, 15LW, and 15LF were used for the finite element analysis of this stacked configuration.

CHAPTER 4

IDENTIFY METHODS OF ANALYSIS

4.1 Commonly Used Methods of Analysis

This section of Chapter 4 presents a modest collection of methods of analysis available to retaining wall designers via literature or passed on from other designers. Since many of the methods currently in use are undocumented, the collection of methods presented here cannot be considered comprehensive.

Not all of the methods presented in Section 4.1 are used to analyze the 64 double-stacked configurations presented in Chapter 3. The second section of this chapter, Section 4.2, identifies which of the methods presented in Section 4.1 will be used to analyze the 64 double-stacked configurations.

4.1.1 Analysis Based on Limit Equilibrium

Several methods of analysis at stacked configurations are based on traditional limit equilibrium theory developed by Rankine or Coulomb. Limit equilibrium theory assumes a Mohr-Coulomb plastic limit soil failure along a planar surface that creates a "failure wedge" of soil. The planar surface is thought to be at an angle to the horizontal that is equal to $45° + \phi / 2$. The force of this failure wedge acting at the backfill face of the retaining wall is then calculated. For the purposes of this thesis, the "active" condition is assumed which assumes that the wall is moving away slightly from the backfill.

4.1.1.1 Equivalent Backfill Slope Method

This method is proposed in a self-published retaining wall design guide by Brooks[2]. The stacked configuration to be analyzed is drawn to scale and the retaining wall designer draws a line which is thought to represent the geometry of the stacked configuration with an "equivalent" slope as shown in Figure 4.1. Then the lower wall is designed as if the upper walls were not present based on the theoretical active earth pressures for "equivalent" slope. Brooks does not define the exact method for determining the location of the line, but some engineers prefer to draw the line such that the "negative" and "positive" areas created by the line are approximately equal, while others prefer to take a sometimes more conservative approach and draw a line which touches the tops of each wall in the stacked configuration, and then approximate an average slope. The active pressure at the lower wall is then calculated based on traditional Rankine or Coulomb theory as if the backfill of the lower wall were sloped along the line of the "equivalent" slope. The upper wall(s) of the stacked configuration are not considered when calculating this increased active pressure at the lower wall. Unlike the three surcharge methods outlined above, this method takes into account the geometry of the stacked configuration. However, note that the active earth pressure at sloped backfill cannot be calculated for "equivalent" slopes with an angle to the horizontal that are greater than the internal angle of friction, ϕ, of the backfill soil.

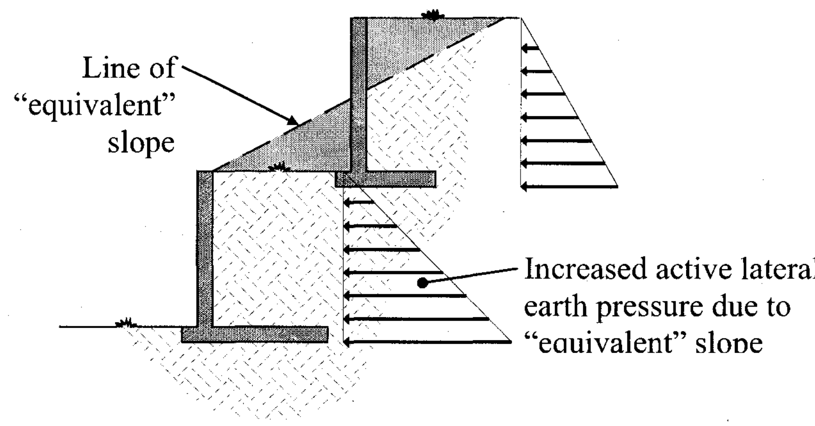

Figure 4.1. Equivalent Backfill Slope Method. Based on the geometry of the stacked retaining wall configuration, the lower retaining wall is designed for an imaginary increased active earth pressure due to an "equivalent" backfill slope.

4.1.1.2 Uniform Surcharge Method

The "Uniform Surcharge Method" was suggested to the author of this thesis by a Las Vegas geotechnical engineer and, like the Equivalent Backfill Slope method of analysis, is also an idealization of the stacked geometry based on limit equilibrium theory. This attempts to account for the additional load of the upper wall(s) at the lower wall of a stacked configuration by applying a uniform surcharge at the backfill of the lower wall equivalent to the weight of a block of the backfill material as shown in Figure 4.2. The surcharge pressure is factored down by the coefficient of active earth pressure, K_a (usually Rankine, but sometimes Coulomb), and applied laterally to the lower wall. This additional lateral pressure calculated due to the imaginary surcharge is then added to the active earth pressure of the lower wall. It should be noted that the active earth pressure at the lower wall is calculated as if it were not included in a stacked configuration, i.e. ignoring the existence of any upper walls. It should also be noted that the weight of the imaginary block of soil is considered only for its contribution to the additional lateral pressure at the lower wall and is otherwise neglected in the design of the lower wall (sliding, overturning, bearing, internal stability, etc.). This method of analysis is generally thought to be conservative. However, as will be shown in the data presented in Chapter 5, this method of analysis does not always result in the most conservative result when applied to the analysis of double-stacked retaining walls. Note that the uniform surcharge method of analysis gives no consideration to the horizontal offset, C, as identified in Figure 3.1 and Table 3.1.

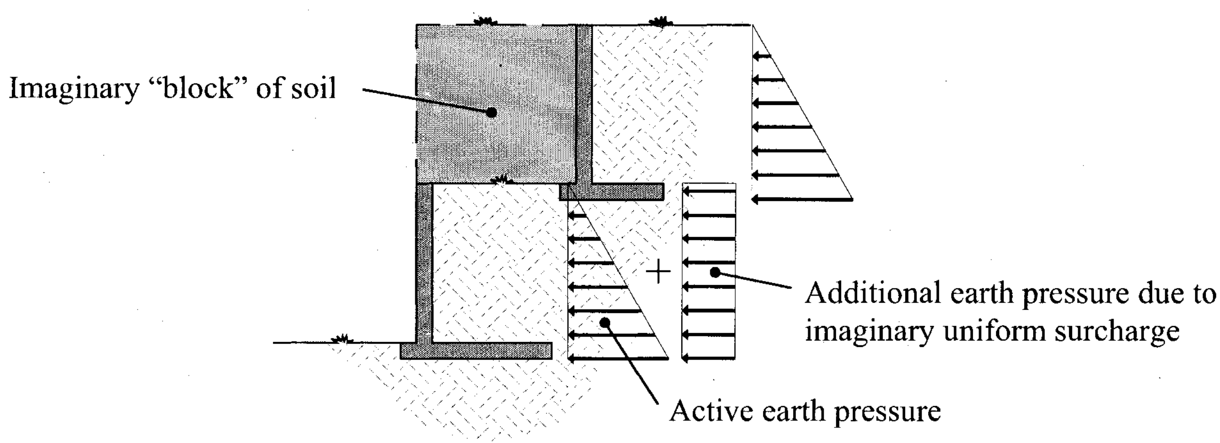

Figure 4.2. Uniform Surcharge Method. Lower retaining wall is designed for surcharge due to the weight of an imaginary "block" of soil that is the same height as the upper retaining wall(s). The weight of the imaginary "block" of soil is not considered to resist overturning of the lower retaining wall.

4.1.1.3 Culmann's Graphical Method

Jean-Victor Poncelet[13, 14] and Karl Culmann[11, 12] are both well-known for their work with graphical methods of analysis to determine lateral earth pressures at retaining walls with compound (level and sloped, radiused, etc.) backfill slopes. Literature linking graphical methods of analysis to the analysis of stacked retaining walls has not been located. However, it is commonly believed that this type of analysis can be applied to complex geometries, such as those of stacked retaining walls. Figure 4.3 provides a schematic of the application of Culmann's graphical method of analysis at a stacked configuration. Culmann's method was developed based on Coulomb's limit equilibrium active earth pressure theory.

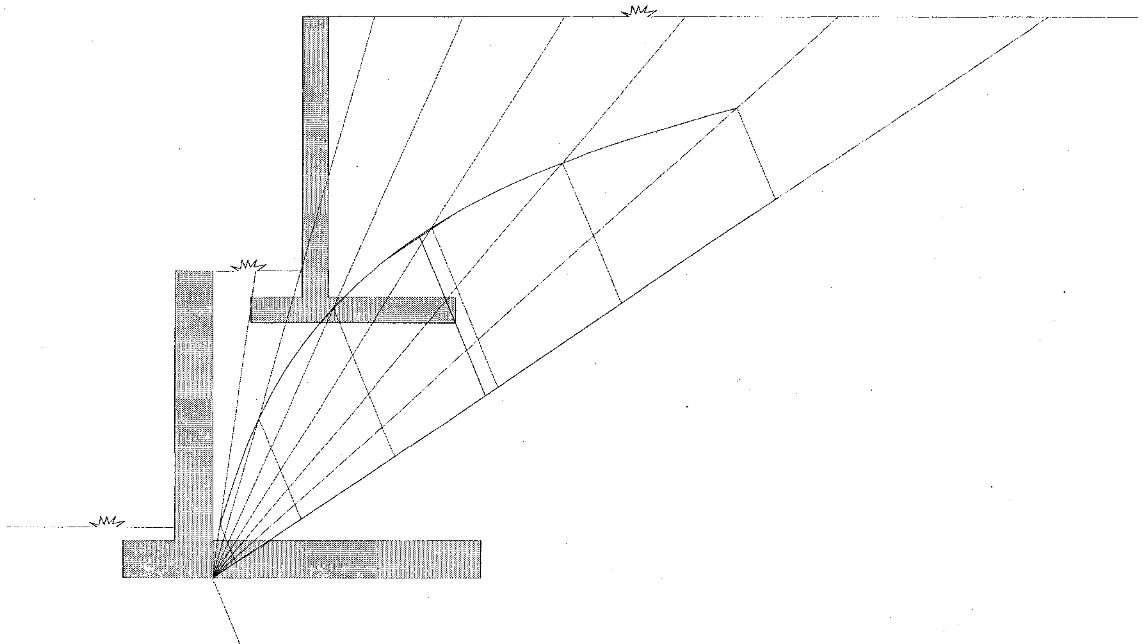

Figure 4.3. Schematic of Culmann's graphical method of analysis

4.1.1.4 Method of Slices

The method of analysis typically referred to as the method of slices is most commonly applied to slope stability analysis. The method of slices differs from other limit equilibrium-based methods of analysis in that the failure surface is not necessarily planar and does not necessarily act at an angle to the horizontal equal to $45° + \phi / 2$.. Textbooks that present the method of slices do not appear to link the method of slices to lateral earth pressure analysis at retaining walls. However, it is commonly believed by retaining wall designers that this method could be applied to retaining wall and stacked retaining wall analysis. Essentially, the analysis is done by assuming a plane of shear failure at the backfill, planar or circular or otherwise, and then dividing the backfill into a number of vertical slices as illustrated in Figure 4.4. The inter-slice force is calculated starting at the slice furthest away from the wall until the force at the interface of the back face of the retaining wall and the slice closest to the wall is determined. Then, a new plane of shear failure is assumed and the process is repeated until the shear plane that results in the highest magnitude of force and the lowest factors of safety is identified. It is believed that the accuracy of this analysis increases with the number of slices and the number assumed shear planes. Many computer applications have been developed to facilitate the use of the method of slices to analyze slope stability, not retaining walls. Some commonly used slope stability analysis applications are XSTABL (Interactive Software Designs, Inc.), Slope-W (GEO-SLOPE International), UTEXAS4 (Shinoak Software), and Slide (Roscience, Inc.).

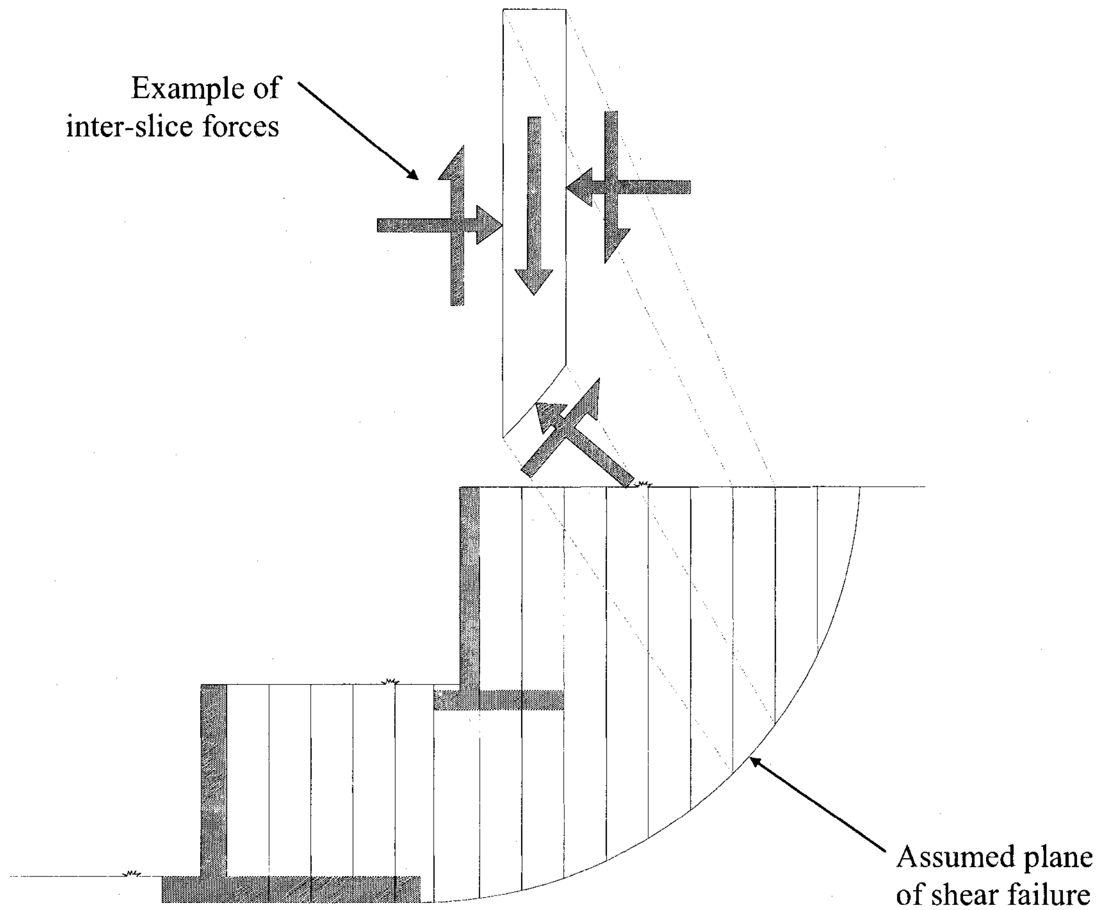

Figure 4.4. Schematic of potential application method of slices to analysis of stacked retaining walls.

4.1.1.5 Olson Method

Olson[3] presents a post-failure analysis of a double-stacked configuration of cantilever retaining walls. Olson's analysis is similar to the method of slices in that a plane of shear failure is assumed and the forces acting on a body of soil are summed until the location and magnitude of the resultant force at the lower wall is calculated. Figure 4.5 presents a schematic of this method of analysis as Olson applies it to the double-stacked configuration. It should be noted that Olson does not provide a name for this type of analysis. However, for convenience of reference to this analysis herein, the term "soil wedge" is used.

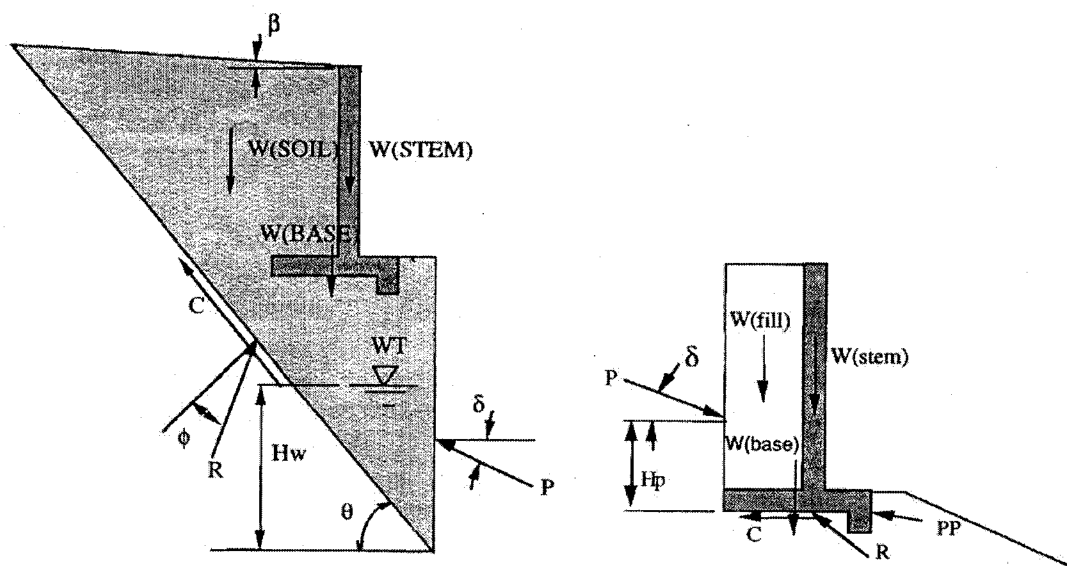

Figure 4.5. Schematic of soil wedge analysis (taken from Olson[3]). A wedge of soil which includes the upper wall is assumed to act on the lower wall.

4.1.2 Analysis Based on Elastic Theory

Methods of analysis based on elastic theory differ from those that are based on limit equilibrium in that no failure is assumed to occur in the soil. Elastic theory is based on the assumptions that the elastic "half-space" of soil behaves in a linear elastic, plane-strain manner. Some methods of analysis at stacked retaining walls appear to have been developed from elastic theory. A few of these are presented in this section.

4.1.2.1 Boussinesq and Others

It appears to be a common practice within the engineering community to idealize the loads from the upper wall(s) as a backfill surface load and then calculate the additional lateral earth pressure at the lower wall based on equations developed from elastic theory. The additional lateral earth pressure resulting from the elastic theory equation is then added to the active lateral earth pressure calculated using traditional Rankine or Coulomb theory as illustrated in Figure 4.6. It is common to idealize the active pressure analysis at the lower wall by ignoring the upper retaining wall(s). It should be noted that during the literature review for this thesis, only one published work by R. Jalla[1] was found to apply elastic theory specifically to the analysis of stacked retaining walls. However, no literature was found during the review for this thesis that validates with experimental data this idealization of loads from upper retaining walls as backfill surface loads.

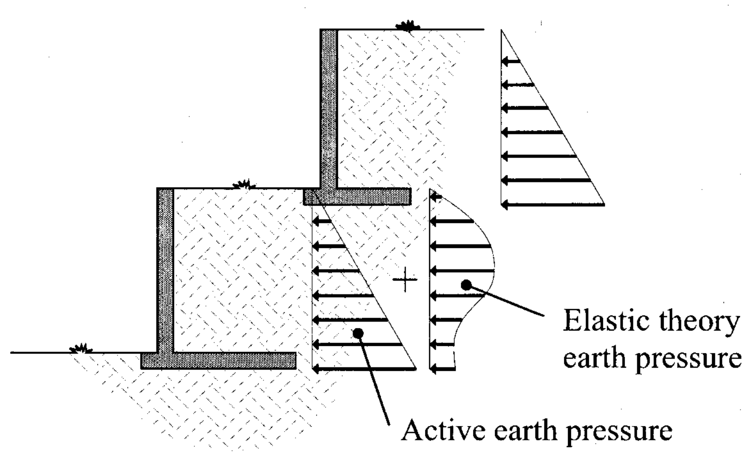

Figure 4.6. Elastic Theory Method of Analysis. Lateral earth pressures at the lower retaining wall(s) are calculated using equations developed from elastic theory, and then added to traditional active earth pressure.

Equations based on elastic theory for horizontal stresses in soil due to backfill surface loads are generally based on the work of French mathematician, J. Boussinesq[6]. The principal equation for lateral stresses due to a point load in an elastic medium as developed by Boussinesq is presented in Figure 4.7. Versions of this equation give lateral stresses due to line loads and strip loads, as well. The published work by R. Jalla[1] proposes a method of analysis of stacked retaining walls based on a version of the elastic theory equation developed by Boussinesq and modified based on the experimental work of Spangler and Mickle[4]. The experimental work of Spangler and Mickle proposes that the Boussinesq lateral pressures due to backfill surface strip loads should be increased by a factor of 2. Bowles[5] notes that the backfill material used by Spangler and Mickle was not compacted and the work was done in the 1930s, prior to the development of modern earth pressure cells. Further Bowles speculates that the uncompacted fill and lack of modern equipment may have contributed to the earth pressures measured at much higher magnitudes than that predicted by elastic theory. It should be noted that solely Jalla links the experimental work of Spangler and Mickle to the analysis of stacked retaining walls. Spangler and Mickle do not provide this link. The experimental work of Spangler and Mickle is limited to the lateral earth pressure due to backfill surface loads, not due to stacked configurations of retaining walls.

There have been others that have expanded upon the elastic theory developed by Boussinesq. Two of the eight methods of analyses presented in Chapter 3 which are used to analyze the 63 different configurations of double-stacked cantilever retaining walls described above are based on elastic theory equations developed by K. Terzhagi[7], and R. Jarquio[8]. Figures 4.8 and 4.8 present these equations. Note that the soil strength parameters, c and ϕ, are not included in equations based on elastic theory. The only parameters are the magnitude of the load at the backfill surface, and geometry of the load relative to the retaining wall.

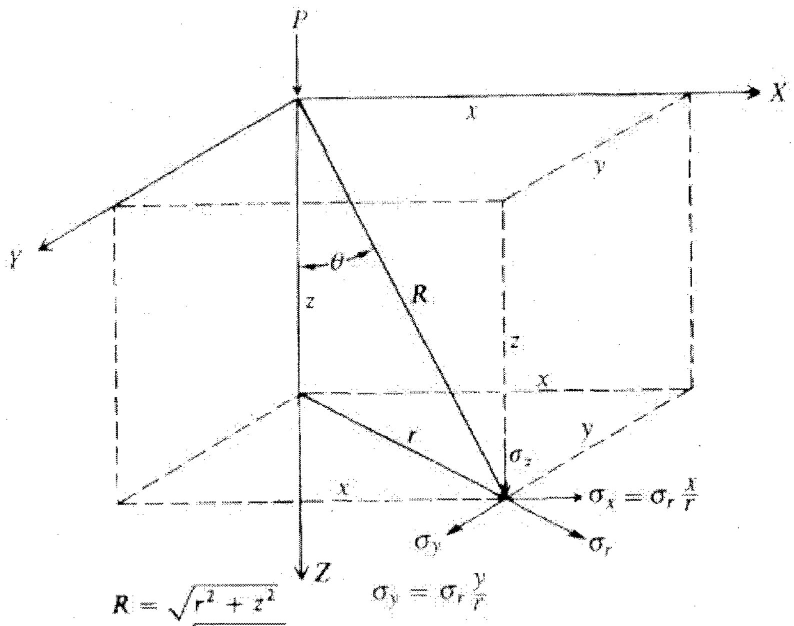

$$R = \sqrt{r^2 + z^2}$$
$$r = \sqrt{x^2 + y^2}$$

$$\sigma_r = \frac{P}{2\pi z^2}\left[3\sin^2\theta\cos^3\theta - \frac{(1-2\mu)\cos^2\theta}{1+\cos\theta}\right]$$

Figure 4.7. The basic form of the Boussinesq Equation based on elastic theory (taken from Bowles[5]).

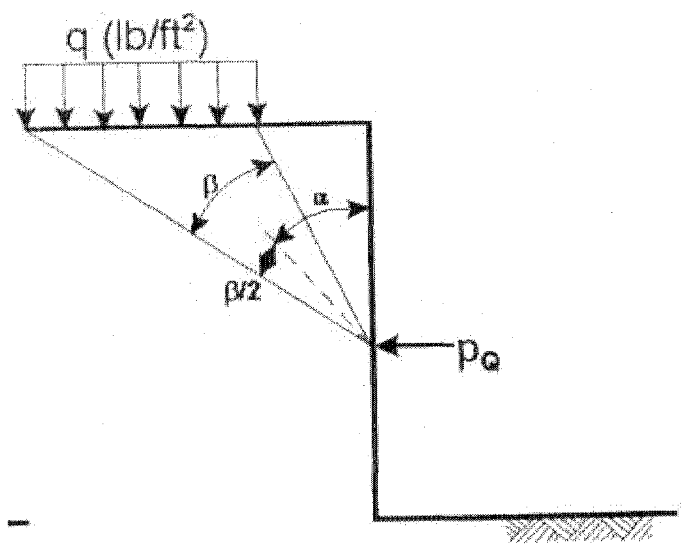

$$p_Q = \frac{2q}{\pi}\left[(\beta + \sin\beta)\sin^2\alpha + (\beta - \sin\alpha)\cos^2\alpha\right]$$

Figure 4.8. Elastic theory-based, experimentally modified equation by Terzaghi[8] for lateral earth pressure due to strip load at the backfill surface (taken from Spigolon[9]).

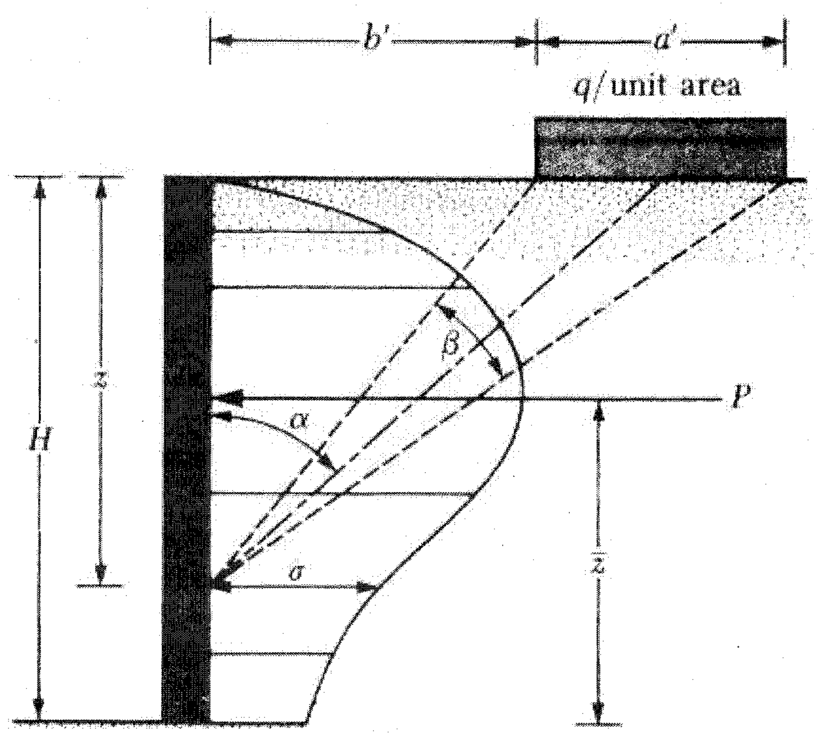

$$\sigma = \frac{2q}{\pi}(\beta - \sin\beta\cos 2\alpha)$$

Figure 4.9. Elastic theory-based equation by Jarqio[7] for lateral earth pressure due to strip load at the backfill surface (taken from Das[10]).

4.1.2.2 Numerical Analysis / Finite Element

As mentioned above, the ideal research for lateral earth pressures at stacked retaining walls is to design and construct several different configurations of stacked retaining walls and instrument them to obtain experimental data, and then used this data to validate a particular method of analysis or develop an altogether new method of analysis. However, the construction and instrumentation of stacked retaining walls is likely a very expensive endeavor, and solicitation for funding of research requiring the construction and instrumentation of such walls may prove to be a difficult task.

Numerical analysis using the finite element method is generally considered to be the "next best thing" to physically obtaining experimental measurements of boundary value problems. It is a common practice among researchers and students in engineering disciplines to compare the results of finite element analysis to the results of more traditional analyses, or to the results of experimentally obtained data. Both practices have validated the use of the finite element method as an alternate to obtaining experimental data. However, it should be noted that for application in this manner, where finite element is used to model an actual condition, it is essential that appropriate site investigation is carried out in order to select soil parameters which will properly model actual conditions. It should also be noted that no published works were encountered during the literature review for this thesis which show the use of the finite element method to analyze stacked retaining walls.

The use of finite element analysis-powered computerized models may help to provide a less expensive alternative to research involving construction and instrumentation of stacked retaining walls to obtain experimental data. Computerized modeling may provide an opportunity to check many more different variables than would construction and instrumentation, resulting in a more comprehensive study. However, at some point the results of the finite element idealizations must be validated against actual field construction.

FLAC (finite difference) and PLAXIS (finite element) are two brands of software commonly used for geotechnical analysis and design. Both of the methods of analysis used by these applications are sophisticated Newtonian-based methods that allow for realistic modeling of problem geometry with a variety of material constitutive models.

While these two brands are common, they are definitely not the only ones available. There are several other finite element applications that specialize in geotechnical analysis and design such as Sigma/W, SAFE, Z_SOIL.PC, CRISP, PENTAGON, SVSOLID. Most have the ability to model soil-structure interaction and can perform two-dimensional or three-dimensional analyses. Others, such as FLAC and PLAXIS, also have the ability to perform a staged analysis which is useful for modeling the effects of construction phasing; an often-overlooked aspect of geotechnical analysis and design.

4.1.3 Analysis Based on Limit Equilibrium and Elastic Theory

In addition to the "Equivalent Backfill Slope Method," a second method of analysis was also proposed by Brooks[2]. This method is reported to have been suggested to Mr. Brooks by a geotechnical engineer, and has been termed "Brooks Surcharge Method" by the author of this thesis and not by Mr. Brooks. Mr. Brooks provides one sentence and a figure to describe this method, however the details of this method are not exactly clear. The following description of this method is an attempt to extrapolate the intent of this method from the sentence and figure provided by Mr. Brooks, and may not represent Mr. Brooks' intent, or the intent of the geotechnical engineer that suggested the method to Mr. Brooks.

The weight of the upper wall(s) and soil is calculated. Mr. Brooks' text then states that the weight of the upper wall(s) is "applied as an adjacent footing"[2] to the lower wall. It is not clear how Mr. Brooks intends for the weight of the wall to be applied "as an adjacent footing" as no example is provided in his guide, but it is assumed that Mr. Brooks is implying that the weight of the upper wall should be considered a uniform backfill surface strip load and the lateral earth pressure due to this strip load is calculated with an equation developed from elastic theory such as that by Jarquio[7] or Terzaghi[8] as described in section 4.2.1. Once the weight of the wall is applied "as an adjacent footing", then it appears that the sliding force at the upper wall is calculated based on traditional Rankine or Coulomb active earth pressure theory. To account for the "horizontal thrust" effects of the upper wall at the lower wall, the resultant of this sliding force at the upper wall is then applied to the lower wall and distributed over the distance, Y, shown in Figure 4.10. Then, the active earth pressure at the lower wall is determined according to Rankine or Coulomb theory. Once this analysis is complete, the lower wall is designed for the lateral earth "pressures" due to the "adjacent footing", and the pressure do to the "horizontal thrust", in addition to the traditional active earth pressure. It is assumed that the active earth pressure at the next wall down from the uppermost wall is calculated as if the wall were not in a stacked configuration. The process is repeated for the next wall down, and on down to the lowermost wall in the stacked configuration. Similar to the Uniform Surcharge Method and the Modified Uniform Surcharge Method, the horizontal geometry, noted as C in Figure 3.1, of the stacked configuration is not considered in the analysis.

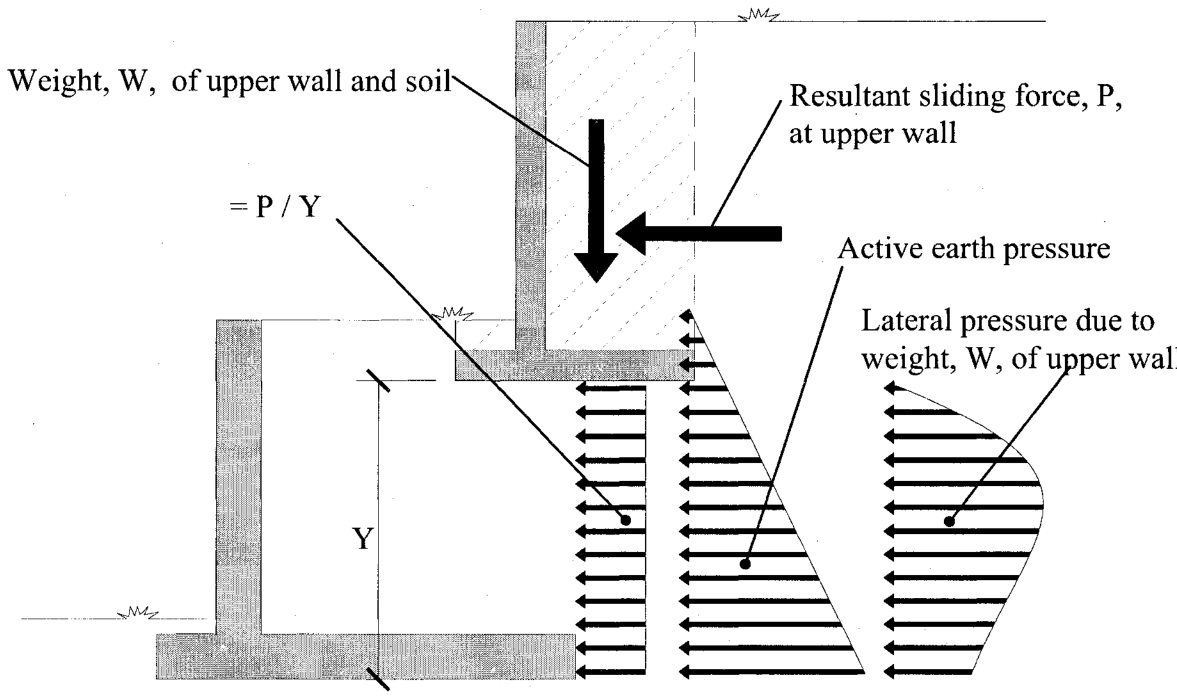

Figure 4.10. Brooks Surcharge Method. Lower retaining wall is designed for surcharge due to the weight, W, and sliding force, P, of the upper retaining wall(s).

4.2 Methods of Analysis Selected for Thesis Study

Only eight of the methods presented in Section 4.1 were used to analyze the 64 different double-stacked configurations. These methods are listed below in Table 4.1. More detailed step-by-step examples for each of these methods are provided in Chapter 5.

Table 4.1. Mark to identify Methods of Analysis in Tables and Figures of results.

Method of Analysis	Mark
Equivalent Backfill Slope (Rankine)	EBS-R
Equivalent Backfill Slope (Coulomb)	EBS-C
Uniform Surcharge	US
Culmann's Graphical	CG
Elastic Theory (Jarquio)	ET-J
Elastic Theory (Terzaghi)	ET-T
Finite Element (Plaxis)	FEA-P
Brooks Surcharge	BS

CHAPTER 5

ANALYSIS OF STACKED CONFIGURATIONS

5.1 Example Analyses of Methods Selected for Thesis Study

This section provides step-by-step examples of how the eight methods selected were used to analyze the 64 different configurations of double-stacked reinforced concrete cantilever retaining walls presented in Chapter 3 (Figures 3.1 and 3.2, Table 3.1). For simplicity, the step-by-step examples are shown for the stacked configuration with the upper and lower wall heights of 5 feet, and a horizontal offset of 5 feet (see Figure 3.1, A = 5 ft, B = 5 ft, and C = 5 ft). For the purposes of this chapter, this particular stacked configuration will be referred to as the 5-5-5 configuration. In all, 512 separate analyses were performed, but this chapter presents only sixteen of these analyses and their results; eight for the 5-5-5 configuration, and eight for the double-stacked configuration that failed in 1992 (Figure 3.2). Results from the remaining 496 analyses along with some interpretation are presented in Chapter 6.

5.1.1 Method 1 Equivalent Backfill Slope (Rankine)

As outlined in section 4.1.1.1, this method requires that the retaining wall designer first draw a section to scale of the stacked configuration. Once this section is drawn, a line of equivalent slope is drawn which is thought to represent the geometry of the stacked configuration and the lower wall is designed based on this slope as if the upper wall(s) do not exist. For the purposes of this thesis, the line representing the equivalent slope will be drawn so that the "positive" and "negative" areas are approximately equal as shown in Figure 5.1. The line of equivalent backfill slope at the 5-5-5 stacked configuration is 29.05 degrees from the horizontal.

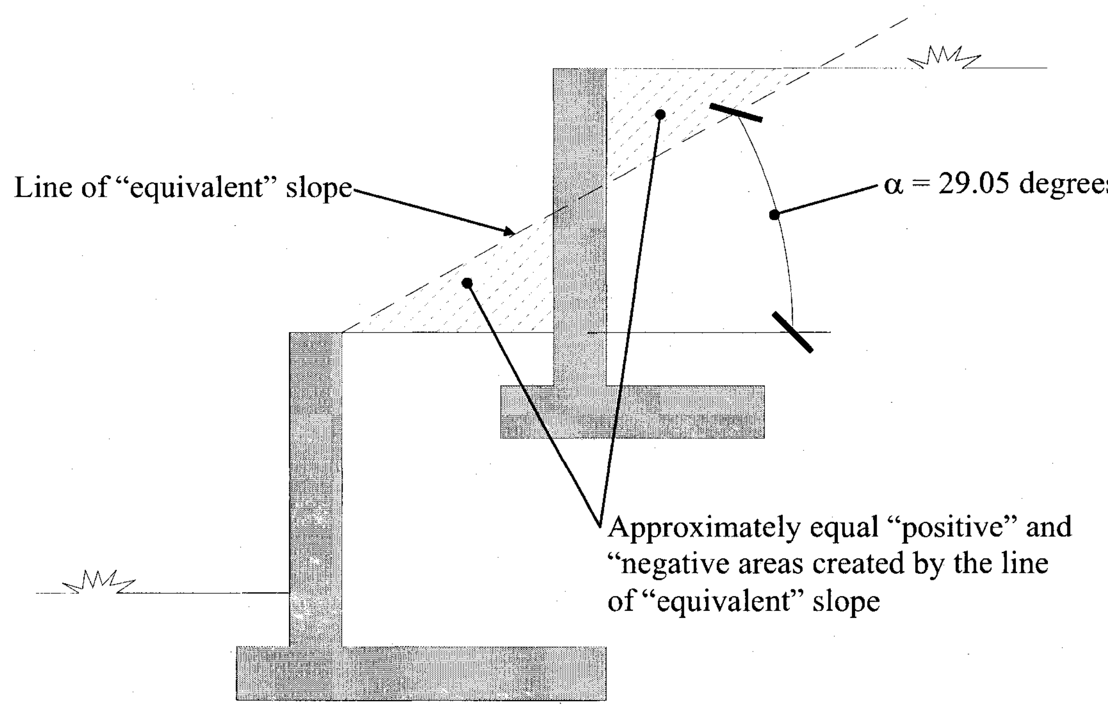

Figure 5.1. Line of equivalent slope at 5-5-5 stacked configuration

According to Rankine theory, the active pressure coefficient, Ka, for sloped backfill is calculated based on the following equation (taken from Das[10]):

$$K_a = \cos\alpha \frac{\cos\alpha - \sqrt{\cos^2\alpha - \cos^2\phi}}{\cos\alpha + \sqrt{\cos^2\alpha - \cos^2\phi}}$$

Where α is the angle from the horizontal of the backfill slope. As shown in Figure 5.1, α is 29.05 degrees for the 5-5-5 stacked configuration, and K_a is 0.453. Thus, the equivalent fluid active earth unit weight, γ_a, is equal to K_a times γ (= 0.453 x 110 pcf), or 49.9 pcf. The sliding force, P, and the overturning moment, M_{ot}, at the lower wall due to γ_a is equal to:

$$P = (\gamma_a H_r^2) / 2 = 1{,}221 \text{ lbs}$$

$$M_{ot} = (\gamma_a H_r^3) / 6 = 2{,}850 \text{ ft-lbs}$$

5.1.2 Method 2 Equivalent Backfill Slope (Coulomb)

The only difference between Method 1 and Method 2 is that the active earth pressure coefficient, K_a, is determined according to Coulomb theory. The primary difference between Coulomb and Rankine theory is that Coulomb accounts for the friction of the soil at the backfill face of the retaining wall, while Coulomb theory ignores this. The active earth pressure coefficient is determined per the following equation (taken from Das[10]):

$$K_a = \frac{\sin^2(\beta + \phi)}{\sin^2\beta \sin(\beta - \delta)\left[1 + \sqrt{\frac{\sin(\phi + \delta)\sin(\phi - \alpha)}{\sin(\beta - \delta)\sin(\alpha + \beta)}}\right]^2}$$

Where β is the angle of the soil face of the retaining wall to the horizontal, α is the angle of the backfill slope to the horizontal, ϕ is the internal angle of friction of the backfill material, and δ is the angle of friction of the backfill soil to the soil face of the retaining wall taken as 2/3 ϕ, and. Thus, Ka is equal to 0.442, and the equivalent fluid active earth unit weight, γ_a, is equal to K_a times γ (= 0.442 x 110 pcf), or 48.6 pcf. The sliding force, P, and the overturning moment, M_{ot}, at the lower wall due to γ_a is equal to:

$$P = (\gamma_a H_r^2) / 2 = 1{,}190 \text{ lbs}$$

$$M_{ot} = (\gamma_a H_r^3) / 6 = 2{,}850 \text{ ft-lbs}$$

Since P is at an angle, δ + 90 degrees, to the soil face of the retaining wall, there is a downward and a horizontal component of this force equal to:

$$P_{down} = P \sin(\delta) = 459 \text{ lbs}$$

$$P_{horiz} = P \cos(\delta) = 1{,}098 \text{ lbs}$$

The downward force due to the friction of the backfill material at the backfill face of the retaining wall, P_{down}, is then added to the system moment resisting.

The calculations for Equivalent Backfill Slope method of analysis for all 64 double-stacked configurations are presented in Appendix B.

5.1.3 Method 3 Uniform Surcharge

As outlined in section 4.1.1.2, the surcharge, q_{sur}, due to an imaginary block of soil equal to the height of the upper wall, $H_{w\text{-}up}$, is factored by K_a (Rankine) and applied to the lower wall as shown in Figure 5.2. The magnitude of the horizontal component of the surcharge load, Pq, and the overturning moment associated with it is equal to:

$$K_a\, q_{sur} = \gamma\, H_{w\text{-}up} = (0.283)\ 110 \text{ pcf} (5 \text{ ft}) = 155 \text{ psf}$$

$$P_q = K_a\, q_{sur} (H_{w\text{-}down} + D_f) = 155 \text{ psf} (5\text{ft} + 2\text{ft}) = 1088 \text{ lbs}$$

$$M_{ot\text{-}q} = [P_q (H_{w\text{-}down} + D_f)^2] / 2 = [155 \text{ psf} (5\text{ft} + 2\text{ft})^2] / 2 = 3{,}810 \text{ ft-lbs}$$

This lateral pressure due to the imaginary surcharge, is then added to the active earth pressure at the lower wall. The active earth pressure at the lower wall is calculated as if the lower wall were not in a stacked configuration. For this thesis, Rankine theory is used to calculate the active earth pressure at the lower wall, but Coulomb could be used just as well. As shown above, K_a is equal to TAN^2 (45° - ϕ / 2) for level backfill slope. For ϕ equal to 34°, K_a is 0.283 and the equivalent fluid active unit weight, γ_a, of the backfill material is equal to γ times K_a, or 31 pcf. The sliding force and overturning moments due to active earth pressure only at the lower wall is:

$$P_a = (\gamma_a H_r^2) / 2 = [31 \text{ pcf} (5 \text{ ft} + 7 \text{ ft})^2] / 2 = 762 \text{ lbs}$$

$$M_{ot\text{-}a} = (\gamma_a H_r^3) / 6 = [31 \text{ pcf} (5 \text{ ft} + 7 \text{ ft})^3] / 6 = 1{,}778 \text{ ft-lbs}$$

This force and moment are then added to the sliding force and overturning moments due to the surcharge load:

$$P_{total} = P_q + P_a = 762 \text{ lbs} + 1{,}088 \text{ lbs} = 1{,}850 \text{ lbs}$$

$$M_{ot\text{-}total} = M_{ot\text{-}q} + M_{ot\text{-}a} = 3{,}810 \text{ ft-lbs} + 1{,}778 \text{ ft-lbs} = 5{,}587 \text{ ft-lbs}$$

The calculations for Uniform Surcharge method of analysis for all 64 double-stacked configurations are presented in Appendix B.

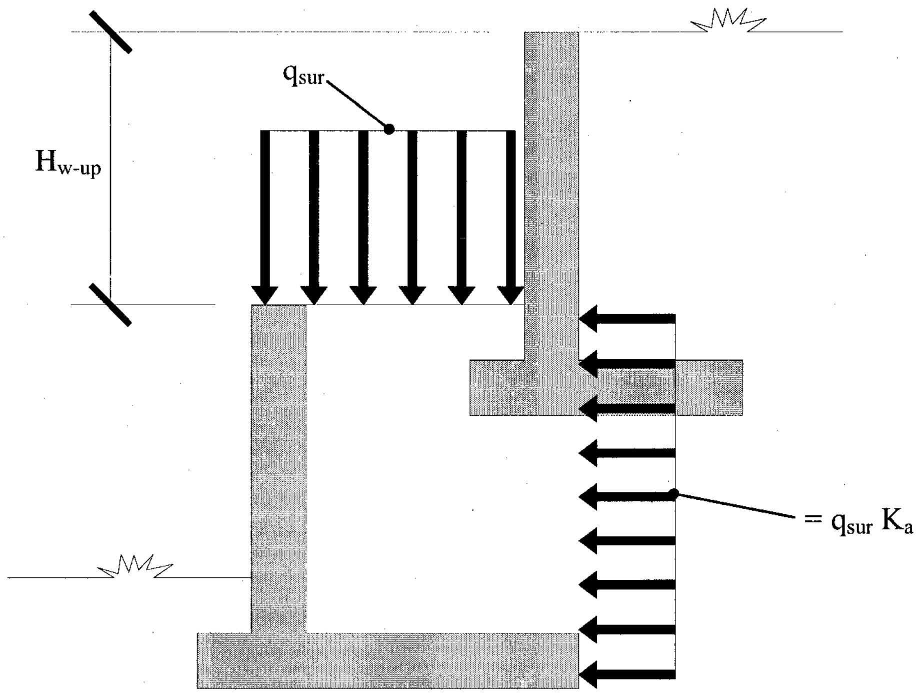

Figure 5.2. Uniform surcharge loads at 5-5-5 stacked configuration.

5.1.4 Method 4 Culmann's Graphical

The steps followed for analysis with Culmann's Graphical Method are provided below along with Figures 5.3 through 5.9 to describe this analysis as it is applies to the 5-5-5 configuration of double-stacked retaining walls. These steps are based on procedures presented by Das[11] but are not presented in the same order. See section 4.1.1.3 for more information regarding this method of analysis.

Note that Das does not link Culmann's graphical method to the analysis of stacked retaining walls. In fact, no literature was encountered during the review for this thesis that links Culmann's or any other graphical method to the analysis of stacked retaining walls.

Step 1. Draw the stacked configuration to scale. The 5-5-5 double-stacked configuration is shown to scale in Figure 5.3.

Step 2. Draw a line that makes angle ϕ with the horizontal as shown in Figure 5.3.

Step 3. Divide the backfill with a polar array of several lines drawn about the intersection of the line of the backfill face of the lower retaining wall and the line drawn in step 2 as shown in Figure 5.4. For the analysis of all 63 stacked configurations, six additional lines at equal increments were drawn.

Step 4. Determine the weight (per foot of length) of the soil / footing / wall bound by the area created by each line and the backfill face of the lower retaining wall. For the 5-5-5 double-stacked configuration, the weights are: 382 plf (pounds per lineal foot), 779 plf, 1506 plf, 2971 plf, 4767 plf, 6983 plf.

Step 5. Pick a convenient scale and plot each weight calculated in step 4 along the step 2 line as shown in Figure 5.5. The plotted weights shown are for the 5-5-5 double-stacked configuration and are to a scale of 1ft :1,000 lbs.

Step 6. Determine the value of the angle, ψ, in degrees: $\psi = 90° - \theta - \delta$, and draw a line that makes angle ψ with the step 2 line as shown in Figure 5.6. The friction angle, δ, is taken as 2/3 of ϕ, and the angle, θ, is the inclination of the backfill face of the retaining wall to the vertical; taken as 0° for all 63 configurations analyzed in this thesis. The value of ψ is $90° - 0° - 2/3(34°) = 67.33°$.

Step 7. Starting at each step 5 point, draw a line parallel to the step 6 line and stop at the step 3 line which corresponds to the boundary of the area used to calculate the weight per foot of the soil / wall / footing as shown in Figure 5.6.

Step 8. Fit a smooth curve that touches the "stop" end of each line drawn in step 7 as shown in Figure 5.6.

Step 9. Draw a line parallel to the step 2 line and tangent to the step 8 curve as shown in Figure 5.7.

Step 10. Starting at the intersection of the step 8 curve and the step 9 line, draw a line that is parallel to the step 6 line as shown in Figure 5.7. The length of this new line is the magnitude of the active force per foot of length at the scale selected in step 5.

Step 11. Draw a line that intersects the end of the step 10 line and the end of the step 2 line as shown in Figure 5.8. This line creates the bottom edge of the Coulomb "failure wedge." The failure wedge for the 5-5-5 double-stacked configuration is shown.

Step 12. Determine the centroid of the failure wedge and draw a line parallel to the step 11 line through the centroid of the failure wedge as shown in Figure 5.9. The intersection of this new line with the backfill face of the lower retaining wall is the approximate point of application of the active force (step 10) due to the failure wedge. There is a more rigorous analytic procedure to determine the true point of application, but according to Das[11], the approximate method described in this step does not sacrifice much accuracy.

The calculations for Culmann's Graphical method of analysis for all 64 double-stacked configurations are presented in Appendix B.

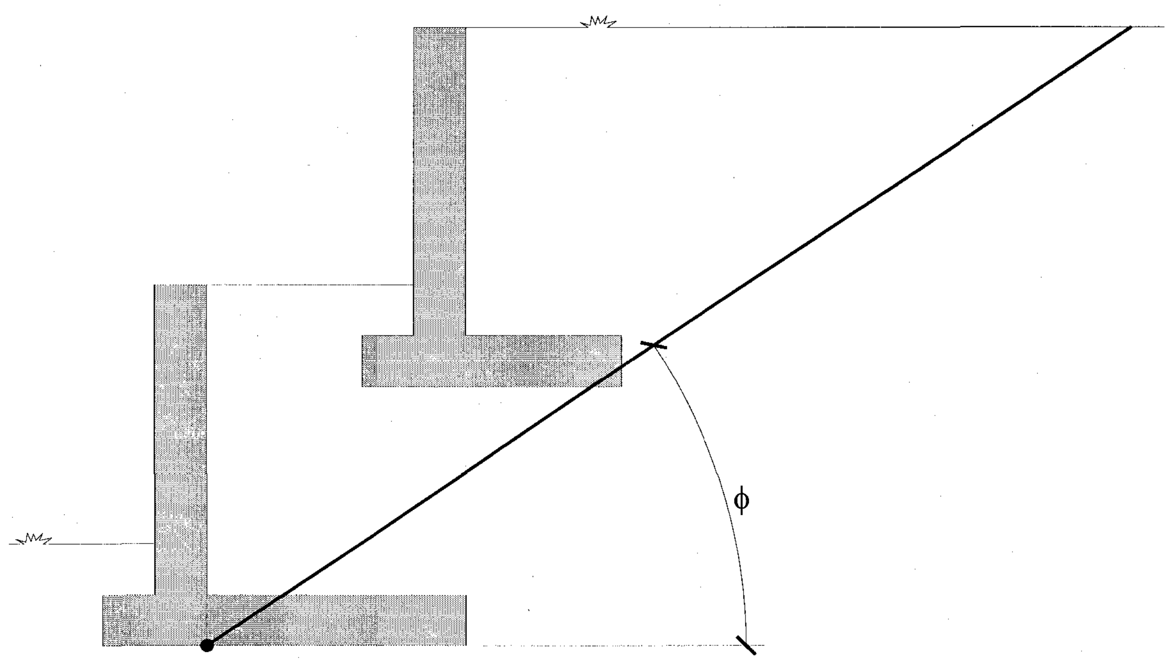

Figure 5.3. Steps 1 and 2 of Culmann's Graphical Method of Analysis.

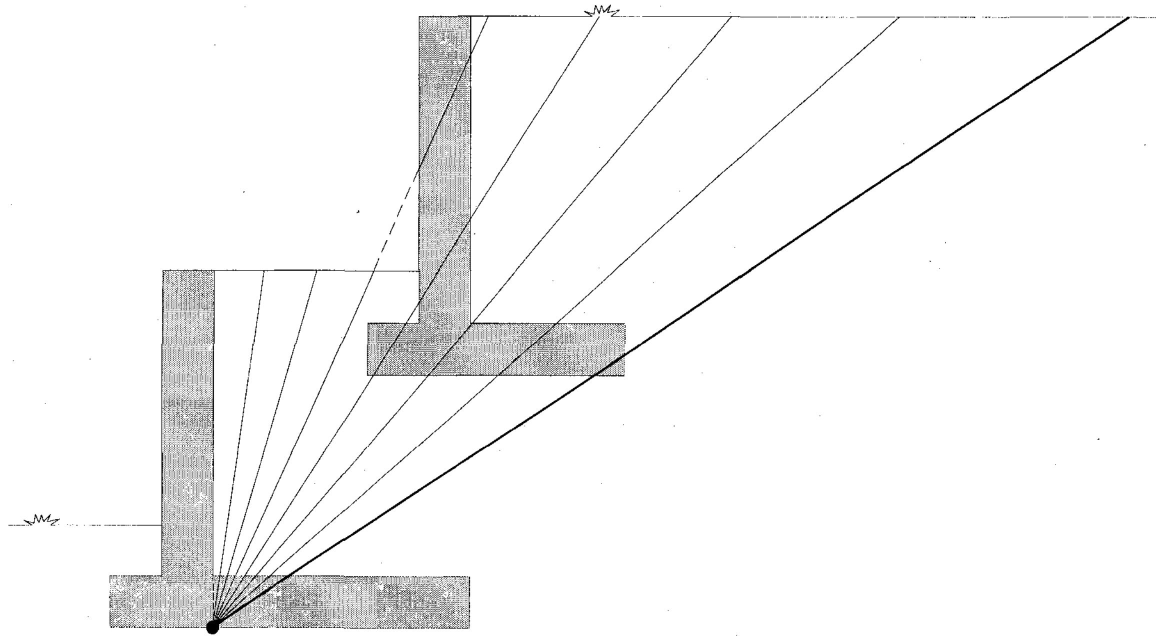

Figure 5.4. Steps 3 and 4 of Culmann's Graphical Method of Analysis.

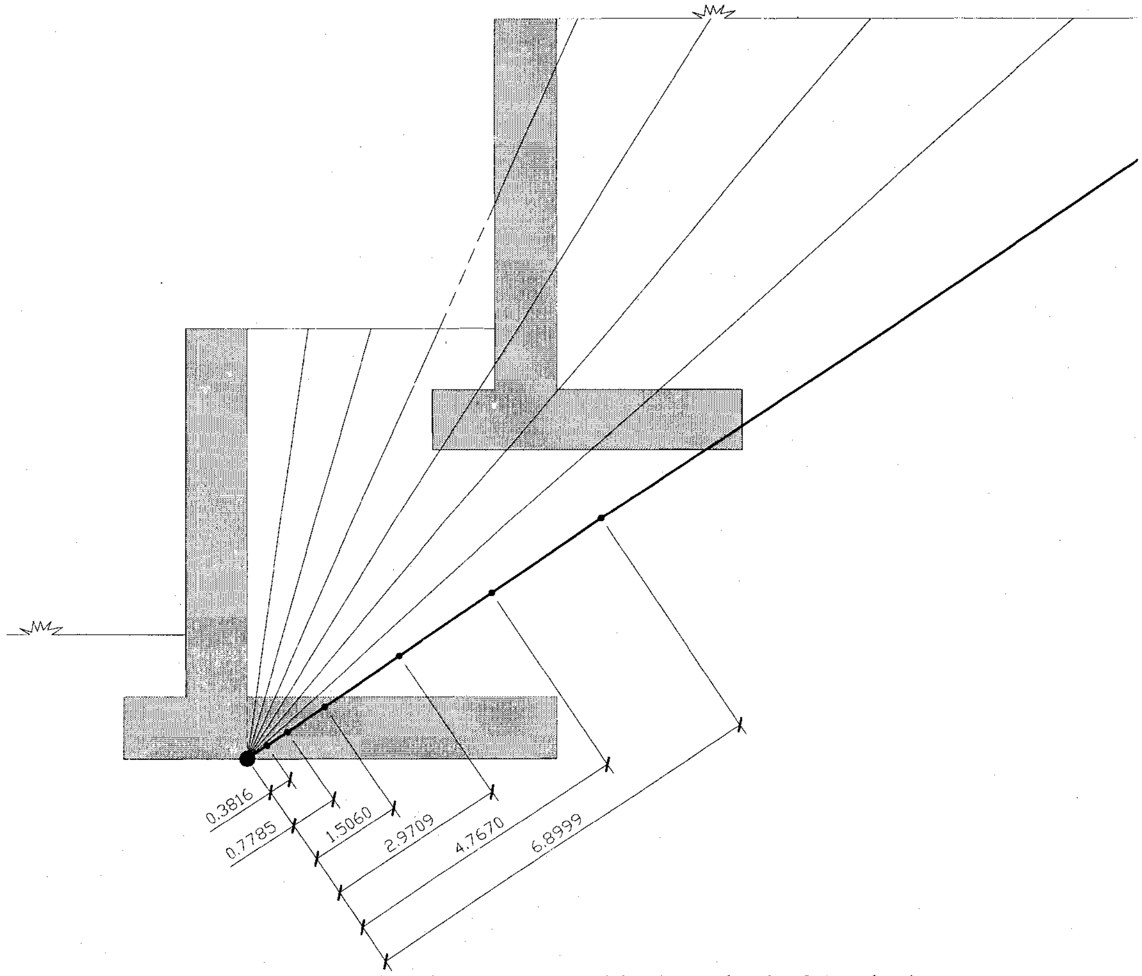

Figure 5.5. Step 5 of Culmann's Graphical Method of Analysis.

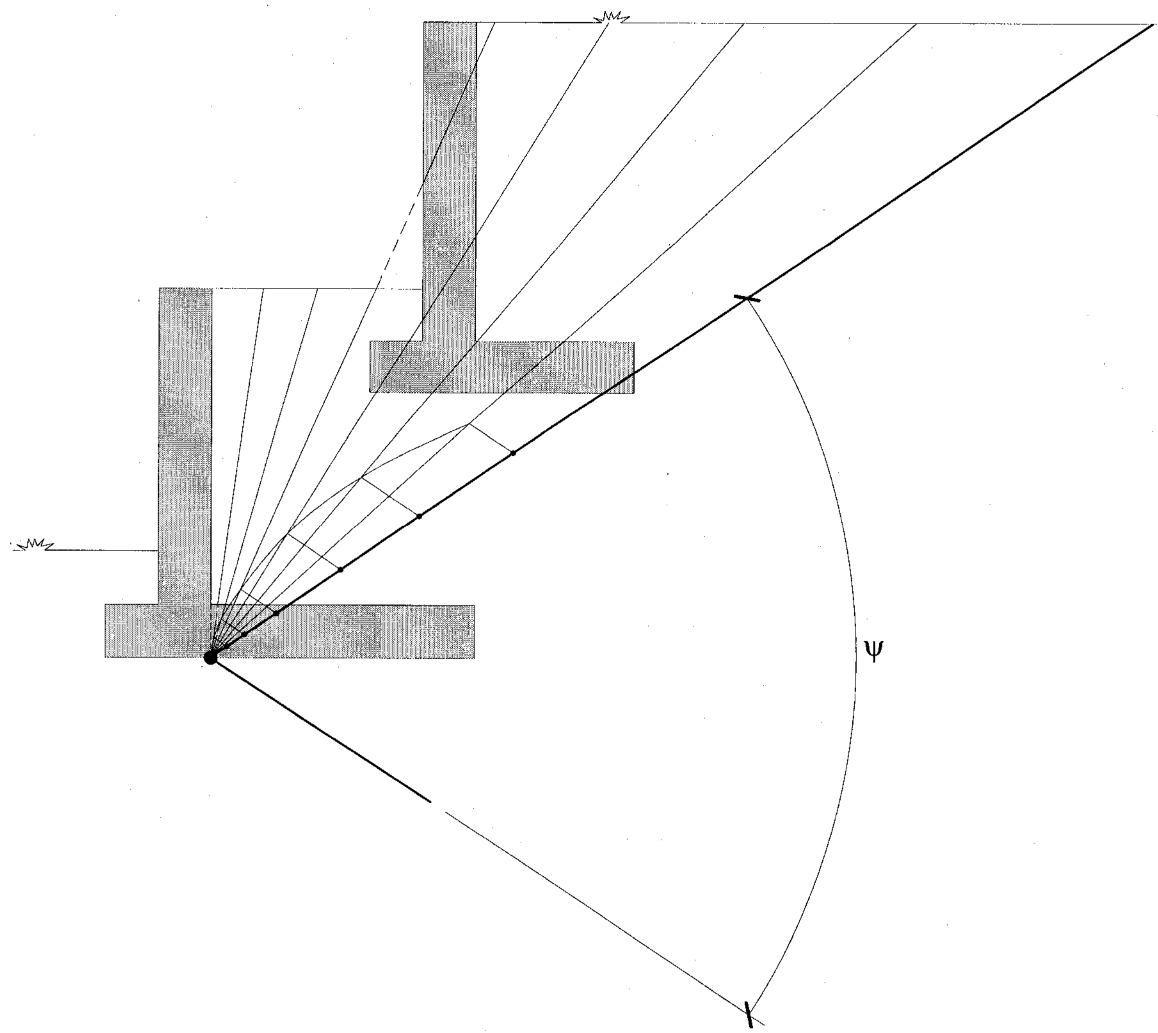

Figure 5.6. Steps 6 through 8 of Culmann's Graphical Method of Analysis.

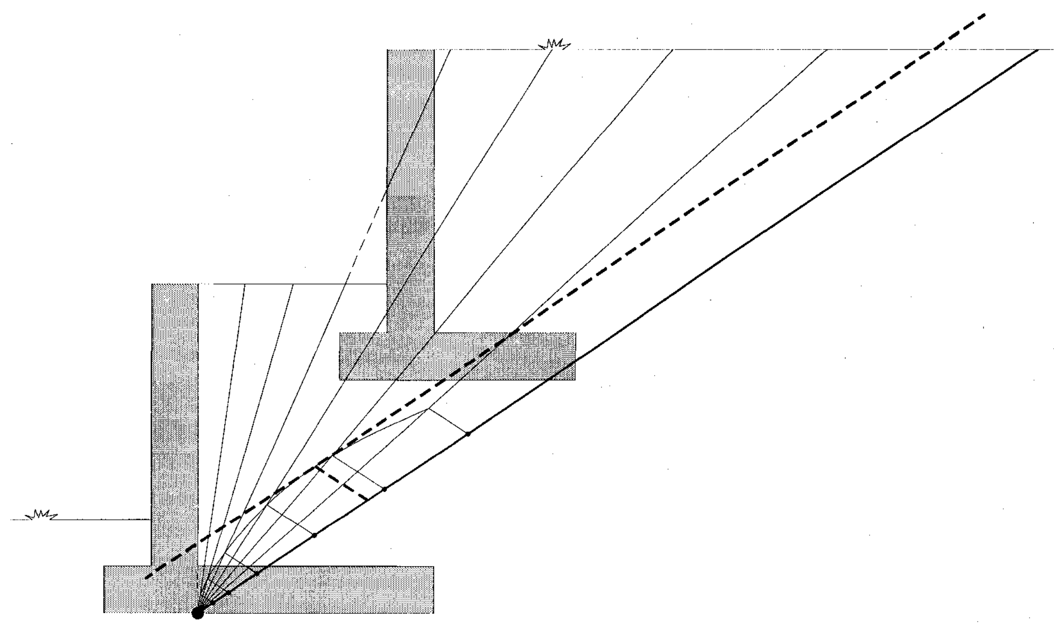

Figure 5.7. Steps 9 and 10 of Culmann's Graphical Method of Analysis.

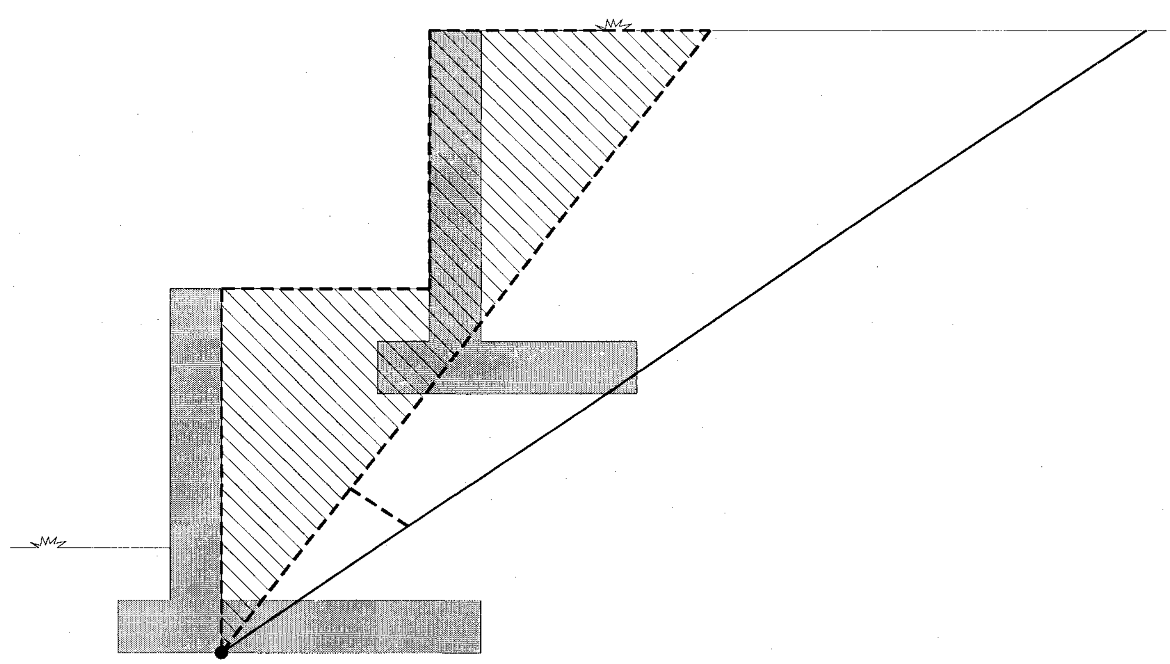

Figure 5.8. Step 11 of Culmann's Graphical Method of Analysis.

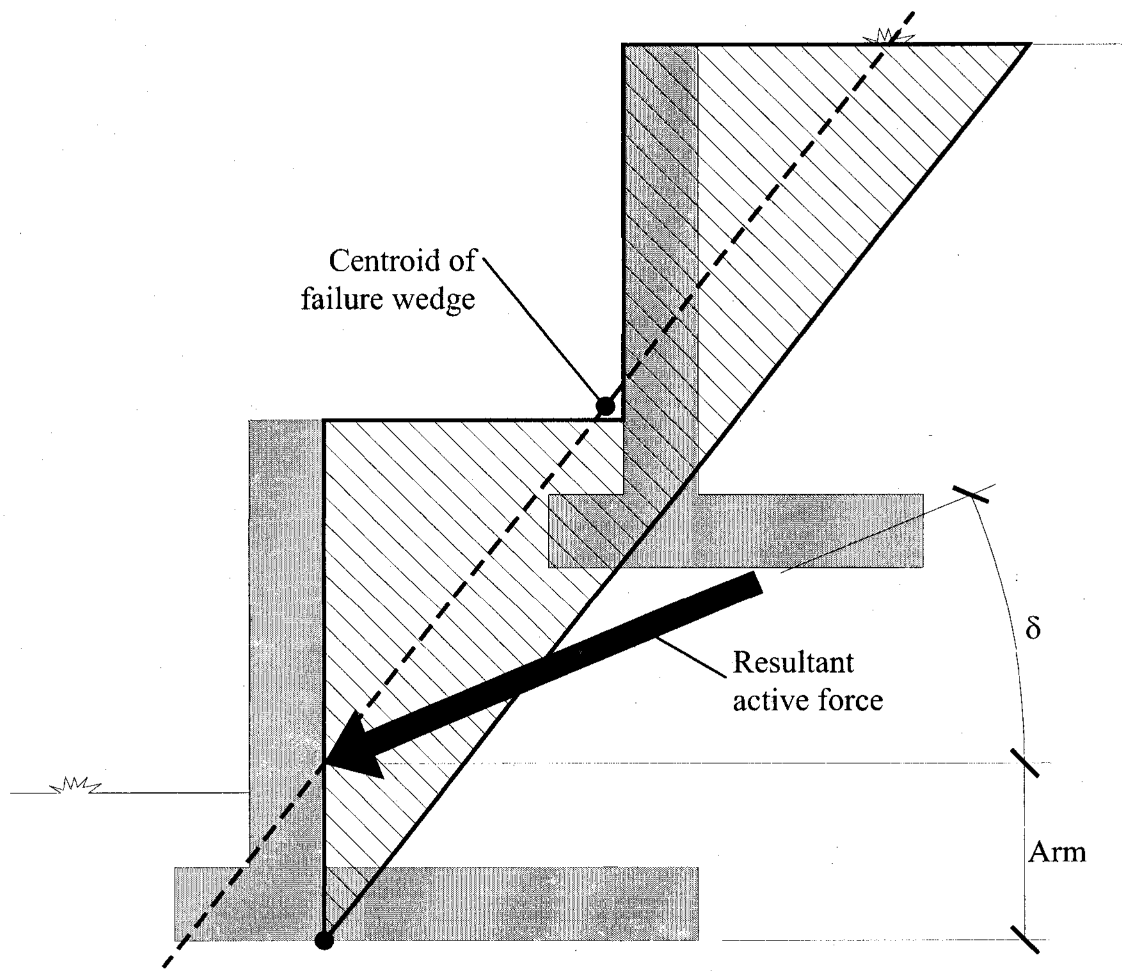

Figure 5.9. Step 12 of Culmann's Graphical Method of Analysis.

5.1.5 Method 5 Elastic Theory (Jarquio)

As shown in Figure 4.9 of Section 4.1.2.1, Jarquio[7] provides a simplified version of the Boussinesq equation for lateral stress due to a backfill surface strip load. This equation results in a stress at a specific elevation. For example, the horizontal stress at the lower wall of the 5-5-5 double-stacked configuration due to the bearing pressure at the upper wall at an elevation of four feet above the bottom of the footing of the lower wall is calculated to be 181 pounds per square foot (psf). At an elevation of two feet above the bottom of the footing of the lower wall the horizontal stress is calculated to be 310 psf. It should be noted that this horizontal stress is due to the average bearing pressure calculated at the footing of the upper wall. For the 5-5-5 configuration, the average bearing pressure at the footing upper wall is 748 psf.

As the results for horizontal stress at different elevations of the lower wall are calculated, a pressure distribution curve is developed. All double-stacked configurations were analyzed for horizontal stress at the lower wall at height increments of 0.75 inches to develop this curve. The magnitude of the area of this horizontal pressure distribution curve is the magnitude of the resultant force, which acts through the centroid of the distribution. For the 5-5-5 configuration, the magnitude of the resultant at the lower wall is 1,207 pounds, and the location of the resultant force is 2.15 feet above the bottom of the footing. Thus, the sliding force and overturning moment at the lower wall associated with the bearing stress from the upper wall is:

$$P_{slide\text{-}elastic} = 1{,}207 \text{ lbs}$$

$$M_{ot\text{-}elastic} = 1{,}207 \text{ lbs } (2.150 \text{ ft}) = 2{,}594 \text{ ft-lbs}$$

The resultant sliding force and overturning moment due to the bearing stress of the upper wall is then added to the sliding force and overturning moment associated with active earth pressure at the lower wall. Similar to the other methods described above which are based on Rankine and Coulomb theory, the active earth pressure is calculated at the lower wall as if there were no upper wall. The sliding force and overturning moment due to this active earth pressure at the lower wall is:

$$P_a = (\gamma_a H_r^2) / 2 = [31.1 \text{ pcf} (5 \text{ ft} + 7 \text{ ft})^2] / 2 = 762 \text{ lbs}$$

$$M_{ot\text{-}a} = (\gamma_a H_r^3) / 6 = [31.1 \text{ pcf} (5 \text{ ft} + 7 \text{ ft})^3] / 6 = 1{,}778 \text{ ft-lbs}$$

The total sliding force and overturning moment at the lower wall is then calculated as:

$$P_{slide\text{-}total} = P_{slide\text{-}elastic} + P_a = 1{,}207 \text{ lbs} + 762 \text{ lbs} = 1{,}969 \text{ lbs}$$

$$M_{ot\text{-}total} = M_{ot\text{-}elastic} + M_{ot\text{-}a} = 2{,}594 \text{ ft-lbs} + 1{,}778 \text{ ft-lbs} = 4{,}372 \text{ ft-lbs}$$

The calculations for earth pressures based on Jarquio Elastic Theory method of analysis for all 64 double-stacked configurations are presented in Appendix C.

5.1.6 Method 6 Elastic Theory (Terzaghi)

This method of analysis is applied to the double-stacked configurations of retaining walls in the exact same manner as presented in Method 5. However, instead of using the equation developed by Jarquio[7], a different equation experimentally developed by Terzaghi[8] is used. The equation developed by Terzaghi, as presented in Figure 4.8, yields results for horizontal stress at a particular elevation just like the equation developed by Jarquio. Thus the calculation methodology used for Method 5 is exactly the same for Method 6.

For the 5-5-5 double-stacked configuration, the resulting sliding force and overturning moment associated with the bearing stress at the footing of the upper is:

$$P_{slide\text{-}elastic} = 1{,}020 \text{ lbs}$$

$$M_{ot\text{-}elastic} = 1{,}020 \text{ lbs } (2.234 \text{ ft}) = 2{,}279 \text{ ft-lbs}$$

The total sliding force and overturning moment at the lower wall of the 5-5-5 double-stacked configuration is calculated as:

$$P_{slide\text{-}total} = P_{slide\text{-}elastic} + P_a = 1{,}020 \text{ lbs} + 762 \text{ lbs} = 1{,}782 \text{ lbs}$$

$$M_{ot\text{-}total} = M_{ot\text{-}elastic} + M_{ot\text{-}a} = 2{,}279 \text{ ft-lbs} + 1{,}778 \text{ ft-lbs} = 4{,}056 \text{ ft-lbs}$$

The calculations for earth pressures based on Terzaghi Elastic Theory method of analysis for all 64 double-stacked configurations are presented in Appendix C.

5.1.7 Method 7 Numerical Analysis / Finite Element (Plaxis)

The finite element software, Plaxis 8.2 Professional Version 2D, was selected to analyze the 64 different double-stacked configurations defined in Figures 3.1 and 3.2, and Table 3.1. Plaxis is designed to specialize in geotechnical applications and features automatic mesh generation and the ability to model stages of construction to produce more realistic models. Plaxis is widely used in geotechnical engineering practice and research, and results from various models have been validated with experimentally obtained data. However, it should be noted that no published work was found during the literature review for this thesis which indicates that results of analysis at stacked retaining walls with Plaxis has been validated with experimentally obtained data.

Elastic theory-based numerical analysis using the finite element computer application, Plaxis, is much more complex than the other methods of analysis presented in this thesis. Finite element analysis requires that much more information be defined regarding the material properties of the soil and the retaining walls. The specifics of the material properties used for the Plaxis finite element analysis is presented in Chapter 3.

Plaxis allows the user to model phases of construction. The initial phase is an existing pit with a scarp on either side at an angle of about 26 degrees (2:1). The first phase is the simulation of the construction of the footing and wall panels of the lower wall. Elastic theory-based analyses are not time dependent, but Plaxis has the ability to "model" time effects of construction phases. Thus a time period of 7 "days" is used for the first phase since it is common to use early high strength concrete for footing and wall panels. The next phases are set up to model backfill the lower wall in twelve-inch lifts. Each lift is estimated to take 0.05 "days" (1.2 "hours") to compete. Once the backfill lifts reach the bottom of the upper wall, then the construction of the upper wall is simulated and is set up for 7 "day" duration like that of the lower wall. Then the backfilling of the upper wall is modeled, also in twelve-inch lifts, until the backfill lifts reach the top of the upper wall. Figure 5.10 shows the twelve-inch high lifts at the 5-5-5 configuration.

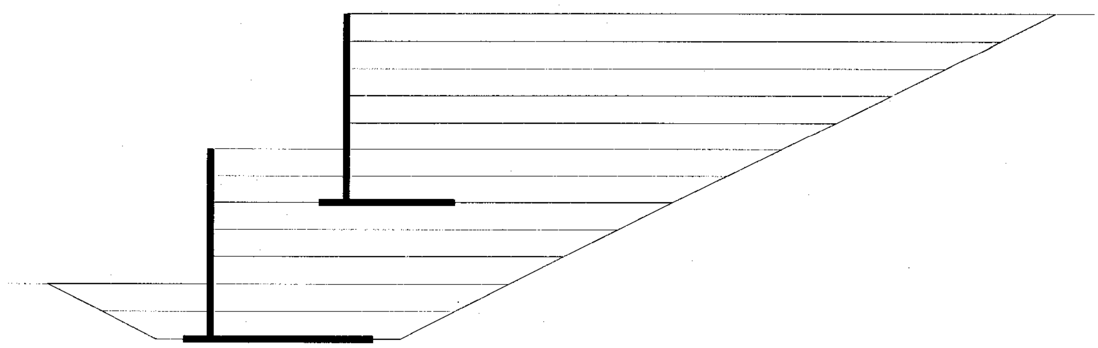

Figure 5.10. Local geometry of 5-5-5 Plaxis model with twelve-inch tall backfill "lifts"

To show that the in-situ stresses prior to the start of the modeling of construction phases are realistic, a point was selected near the bottom of the model and the ratio of the vertical stress, σ_v, to the horizontal stress, σ_h, was calculated. This ratio, referred to as K_o, was calculated to be around 0.44 for all models. This value for K_o is realistic.

The overall geometry plays a role in the results produced by Plaxis. When a Plaxis model is created, Plaxis prompts the user to input the overall dimensions of the model. For example, the geometry of the 5-5-5 double-stacked configuration is measured ten feet horizontally from toe of lower wall to heel of upper wall and twelve feet vertically from bottom of footing at the lower wall to top of wall at the upper wall. However, the minimum overall geometry of the model created in Plaxis is 142 feet horizontally by 60 feet vertically. Since each not every double-stacked configuration is the same overall height, the overall dimensions of the Plaxis model needed to be considered. After several trial iterations, it was determined that the overall geometry of each Plaxis model should be proportioned the same based on the overall height of the configuration of the double-stacked retaining walls. Figure 5.11 is provided to demonstrate the minimum proportions used in all the Plaxis models created for this thesis.

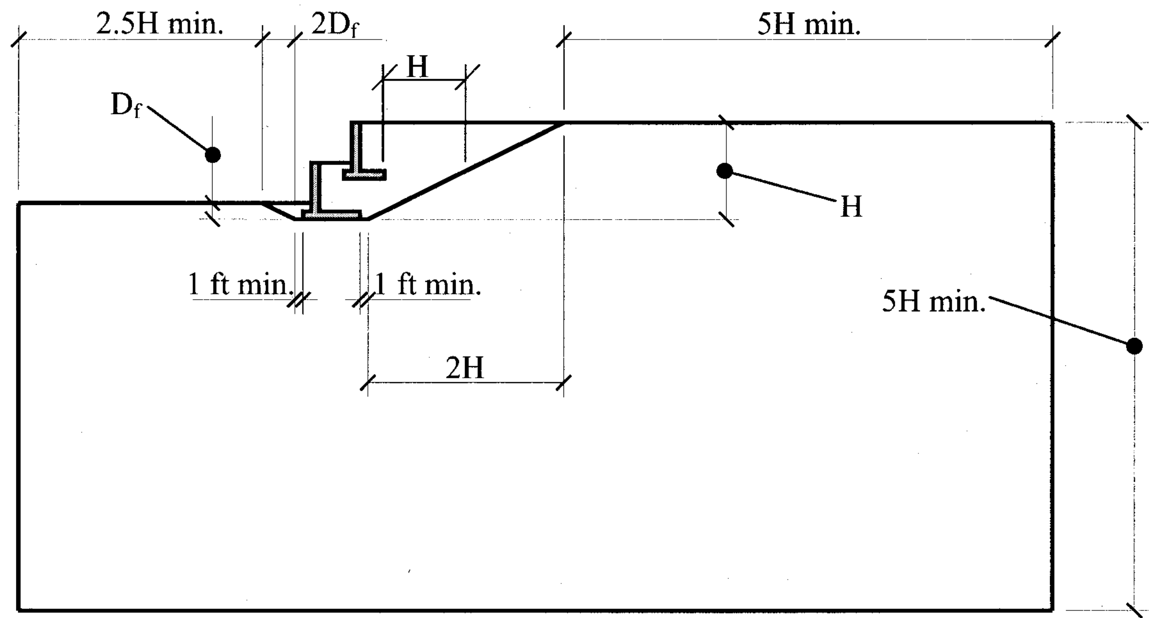

Figure 5.11. Overall geometry proportions used in the Plaxis models created for the 63 double-stacked configurations.

The effect of the height of the backfill lifts was explored. The first model to demonstrate this was set up so that the backfill and subgrade material were all one continuous block of soil. Then a model was created where the backfill was separate from the subgrade material, but the backfill was one block of soil. Then a model was created with the backfill divided into two lifts separated at the bottom of the upper retaining wall. Then a model was created that separated the backfill into four "lifts". This process was repeated until the lifts were about twelve inches high. The results of the lateral pressure distribution converge with the addition of simulated lifts. Therefore, the use of twelve-inch lifts is believed to better model actual conditions.

Plaxis allows the user to set the coarseness of the mesh. Unlike some finite element applications, Plaxis has a feature that will automatically generate the mesh. It is generally believed that actual conditions are better modeled with less course mesh. The mesh generated by Plaxis was set to the highest density setting of "very fine" for all 63 models of the double-stacked configurations.

Plaxis also allows the user the view the deformations. Deformations are dependent upon Young's Modulus, E, of the soil. According to Bowles[5], Young's Modulus for sand is typically 150,000 psf on the low end at silty sand, and 1,700,000 psf on the high end at dense sand. A value of 1,000,000 psf was selected for E that is on the low end of values for dense sand. It should be noted that the highest value for total extreme deformation (combined horizontal and vertical) output by Plaxis with this value of E applied to the double-stacked configurations, not including the 1992 failure double-stacked configuration, was 3.4 inches at the 15-15-7.5 configuration. The total deformation at the 5-5-5 configuration was only 0.4 inches.

The footing and wall panels of the retaining walls were modeled in Plaxis as plates with a soil-structure interface according to the recommendations provided in the tutorials. These plates are represented by just a line in the model with no thickness. Plaxis allows the user to draw a section through the model and graphically view the output of the lateral pressure at the rear face of the lower retaining wall as shown in Figures 5.12 and 5.13. In order to obtain results that were comparable to the results obtained with the other methods of analysis, the plate lines were conservatively drawn at the front face of the walls, and the bottom face of the footings. The more structurally correct method of modeling the retaining walls is to draw the plates at the centerline of the wall and footing panel thickness. Several models were created with the plates at the centerline of the footing and panel thickness. The output of these analyses was compared to the output with the plates drawn at the wall front face and footing bottom face. The resultant of the horizontal pressure distributions with the plates at centerline were, of course, about ten to fifteen percent lower in magnitude than those with the plates drawn at front and bottom faces of the panels. However, for the purposes of comparing the results of the Plaxis models to the other methods of analysis, the models for the 64 double-stacked configurations were drawn with the plates at the front and bottom faces of the wall and footing panels.

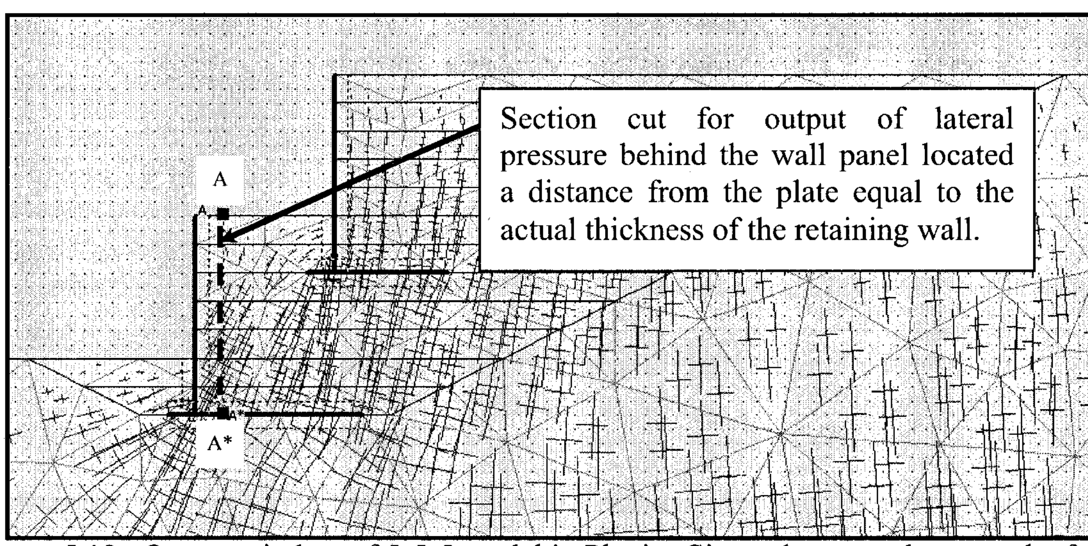

Figure 5.12. Output window of 5-5-5 model in Plaxis. Since plates are drawn at the front face of the wall, and the bottom face of the footing, cross section A-A* is cut a distance from the plate line that is equal to the thickness of the lower wall. See Figure 5.13 for output of cross section A-A* lateral earth pressure distribution and resultant magnitude and location.

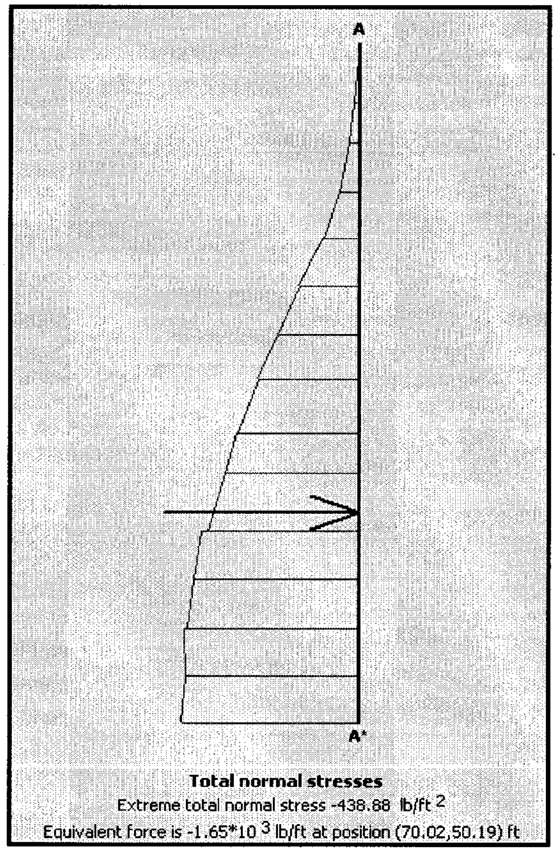

Figure 5.13. Horizontal pressure distribution, and resultant magnitude and location (1,650 plf at 2.19 ft above the bottom of footing) at section A-A* of the 5-5-5 configuration cut at the location shown in Figure 5.12.

The lateral pressure distribution output, similar to that shown in Figure 5.13, for all 64 double-stacked configurations is provided in Appendix E.

5.1.8 Method 8 Brooks Surcharge

As outlined in section 4.1.3, Brooks[2] presents a method of analysis, which combines traditional Rankine/Coulomb active earth pressure theory with elastic theory. The objective of this method appears to be based on a separate theory that, in addition to increased lateral earth pressure at the lower wall due to the vertical loads of the upper wall, a "horizontal thrust" due to the sliding force at the upper wall(s) also acts on the lower wall(s) in a stacked configuration as shown in Figure 4.10.

For the purposes of this thesis, the additional horizontal stresses at the lower wall of the 5-5-5 double-stacked configuration due to the bearing pressure of the upper wall is calculated in accordance with Method 5 as shown in section 5.5 and shown below for reference. Method 6, or any other method based on elastic theory could have just as well been used as Brooks[2] does not specify that a particular method be used.

$$P_{slide\text{-}elastic} = 1{,}207 \text{ lbs}$$

$$M_{ot\text{-}elastic} = 1{,}207 \text{ lbs } (2.150 \text{ ft}) = 2{,}594 \text{ ft-lbs}$$

$$P_a = (\gamma_a H_r^2) / 2 = [31 \text{ pcf } (5 \text{ ft} + 7 \text{ ft})^2] / 2 = 762 \text{ lbs}$$

$$M_{ot\text{-}a} = (\gamma_a H_r^3) / 6 = [31 \text{ pcf } (5 \text{ ft} + 7 \text{ ft})^3] / 6 = 1{,}778 \text{ ft-lbs}$$

$$P_{slide\text{-}total} = P_{slide\text{-}elastic} + P_a = 1{,}207 \text{ lbs} + 762 \text{ lbs} = 1{,}969 \text{ lbs}$$

$$M_{ot\text{-}total} = M_{ot\text{-}elastic} + M_{ot\text{-}a} = 2{,}594 \text{ ft-lbs} + 1{,}778 \text{ ft-lbs} = 4{,}372 \text{ ft-lbs}$$

The sliding force at the upper wall is calculated based on traditional Rankine active earth pressure theory. The coefficient of active earth pressure, K_a, according to Rankine theory is equal to $\text{TAN}^2 (45° - \phi / 2)$ for level backfill slope. For ϕ equal to 34°, K_a is 0.283 and the equivalent fluid active unit weight of the backfill material is equal to γ_a times K_a, or 31.1 pcf. Thus, the sliding force at the upper wall of the 5-5-5 double-stacked configuration is shown below. The terms H_w and D_f at the upper wall are defined in Figure 3.3 and Table 3.2 in section 3.3.

$$P_{slide\text{-}upper} = [\gamma_a (H_w + D_f)] / 2 = [31 \text{ pcf} (5\text{ft}+2\text{ft})] / 2 = 762 \text{ lbs}$$

This sliding force is then distributed as a uniform pressure at the lower wall over a distance, Y, as shown in Figure 4.10. Since this horizontal pressure is considered to be a uniform distribution, the resultant of this sliding force due to the upper wall acts at a distance equal to half of Y above the bottom of the footing of the lower wall. The overturning moment at the lower wall associated with the "horizontal thrust", $P_{slide\text{-}upper}$, at due to the upper wall is calculated as shown below:

$$M_{thrust} = P_{slide\text{-}upper} (Y/2) = 762 \text{ lbs} (5 \text{ ft} / 2) = 1{,}905 \text{ ft-lbs}$$

The sliding force and overturning moment at the lower wall due to the bearing pressure and "horizontal thrust" effects of the upper wall are then added to the sliding and overturning force associated with active earth pressure at the lower wall. Similar to the other methods described above which are based on Rankine and Coulomb theory, the active earth pressure is calculated at the lower wall is calculated as if there were no upper wall. The sliding force and overturning moment due to this active earth pressure at the lower wall is:

$$P_a = (\gamma_a H_r^2) / 2 = [31.1 \text{ pcf} (5 \text{ ft} + 7 \text{ ft})^2] / 2 = 762 \text{ lbs}$$

$$M_{ot\text{-}a} = (\gamma_a H_r^3) / 6 = [31 \text{ pcf} (5 \text{ ft} + 7 \text{ ft})^3] / 6 = 1{,}778 \text{ ft-lbs}$$

The total sliding force and overturning moment at the lower wall of the 5-5-5 double-stacked configuration is calculated as:

$$P_{slide\text{-}total} = P_{slide\text{-}elastic} + P_{slide\text{-}upper} + P_a = 1{,}207 \text{ lbs} + 762 \text{ lbs} + 762 \text{ lbs} = 2{,}730 \text{ lbs}$$

$$M_{ot\text{-}total} = M_{ot\text{-}elastic} + M_{thrust} + M_{ot\text{-}a} = 2{,}594 + 1{,}905 + 1{,}778 = 4{,}056 \text{ ft-lbs}$$

The calculations for Brooks Surcharge method of analysis for all 64 double-stacked configurations are presented in Appendix B.

5.2 Analysis of a Post-Failure Case Study

Olson[3] authored a report of a post-failure analysis of a double-stacked configuration of cantilever concrete retaining walls. The report provides fairly detailed information regarding the geometry of the individual walls and the overall stacked configuration, and the material properties of the soil. The report also presents the results of an analysis of the double-stacked configuration. Figure 3.2 shows the geometry of the stacked configuration.

This configuration has been analyzed using the eight methods of analysis applied to the 63 stacked configurations as described above in this chapter. The soil properties assumed for this analysis are shown in Table 5.1. Not all of the soil properties are available in Olson's report.

Table 5.1. Soil properties assumed for analysis of case study retaining wall.

Material Property	Description	Value
γ_{unsat}	Unsaturated Unit Weight of Soil	110 pcf
γ_{sat}	Saturated Unit Weight of Soil	130 pcf
k_x	Permeability in the x direction	3 ft/day
k_y	Permeability in the y direction	3 ft/day
E	Young's Modulus	100,000 psf
ν	Poisson's Ratio	0.27
c	Soil Cohesion	0.05 psf
ϕ	Angle of Internal Friction	25°

CHAPTER 6

RESULTS

6.1 Results of Thesis Study

Results from the analyses described above are presented in this section. The eight different methods presented in Section 4.2 were used analyze the 63 configurations of double-stacked walls presented in Chapter 3 for the thesis study which does not include the configuration of the double-stacked retaining walls that failed in 1992. For the purposes of presenting this results of these 504 analyses, refer to Table 4.1 for a legends of marks used to identify methods of analysis in the tables and figures that follow.

The double-stacked configurations will be identified in the same manner that the 5-5-5 configuration was identified in section 5.1: (retained height of the lower wall)-(retained height of the upper wall)-(horizontal offset). For example, the mark 10-5-17.5 refers to the double-stacked configuration where the retained height of the lower wall (identified as A in Figure 3.2) is ten feet, the retained height of the upper wall (identified as B in Figure 3.2) is five feet, and the horizontal offset (identified as C in Figure 3.2) is 17.5 feet.

It is generally assumed by retaining wall designers that the closer the upper wall of a double-stacked configuration is located to the lower wall, the higher the magnitude of the sliding force and overturning moment at the lower wall, and the lower the factors of safety against sliding and overturning. The results of analysis of the 63 double-stacked configurations seem to follow this assumption for all eight methods of analysis with the exception of the Uniform Surcharge (US) method. Figures 6.1 and 6.2 show that the sliding force and overturning moment generally increase as the horizontal spacing between the stacked walls decreases at the 5-5-5 double-stacked configuration. Figures 6.3 and 6.4 show that the factors of safety against sliding overturning generally decrease as the horizontal spacing between the stacked walls decreases at the 5-5-5 double-stacked configuration. Charts have been developed similar to the chart presented in Figure 6.1 for all 63 double-stacked configurations of the thesis study and are located in Appendix G of this thesis. Refer to Table 4.1 for a legend of the marks used to note the methods of analysis (EBS-R, EBS-C, US, etc.).

Sliding Force for Double-Stacked Configuration: A = 5 ft and B = 5 ft

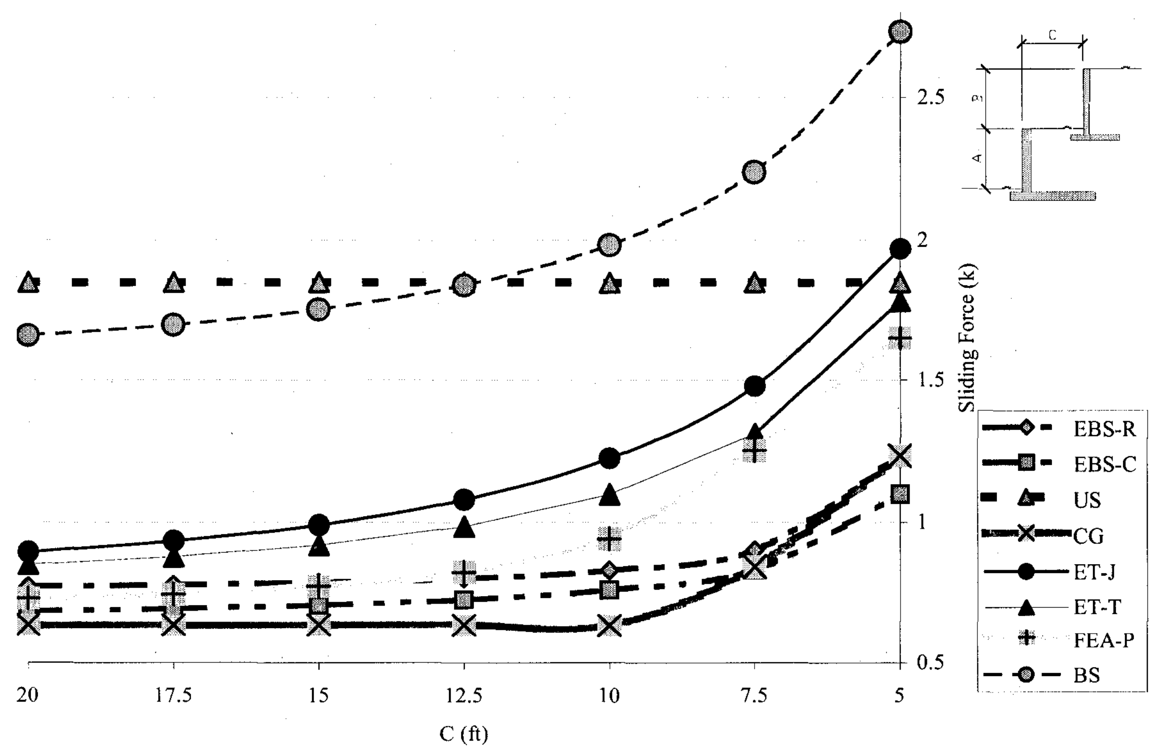

Figure 6.1. Sliding force with respect to horizontal offset, C, at double-stacked configuration where height of upper and lower walls, B and A, is 5 feet.

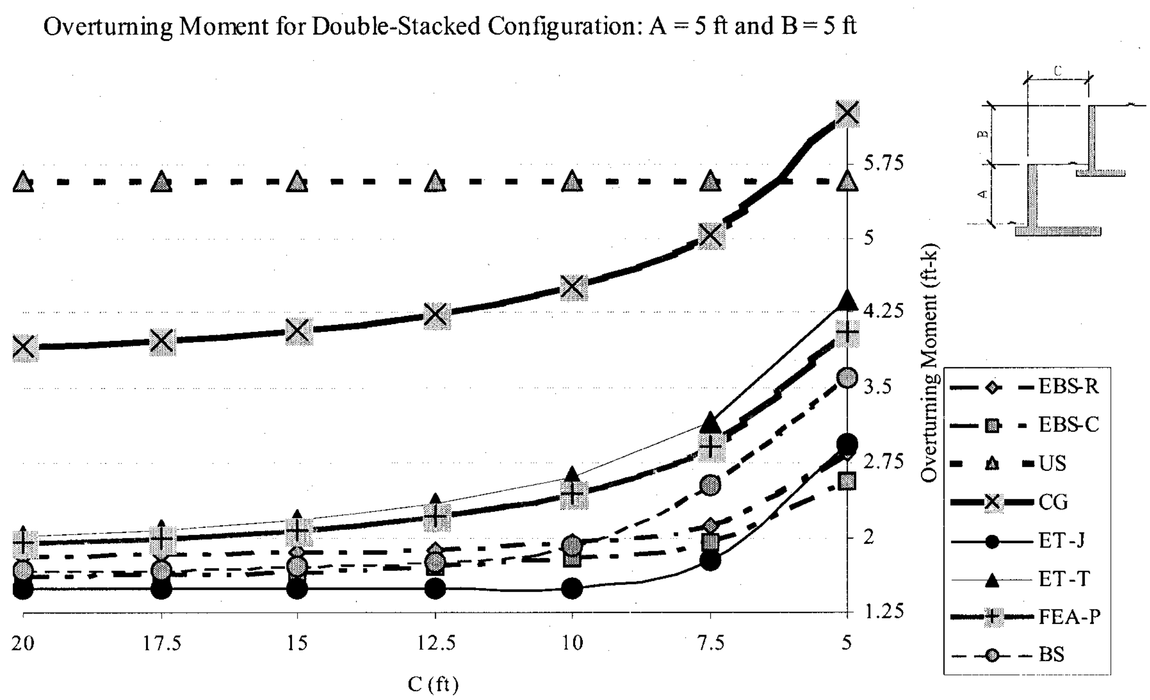

Figure 6.2. Overturning moment with respect to horizontal offset, C, at double-stacked configuration where height of upper and lower walls, B and A, is 5 feet.

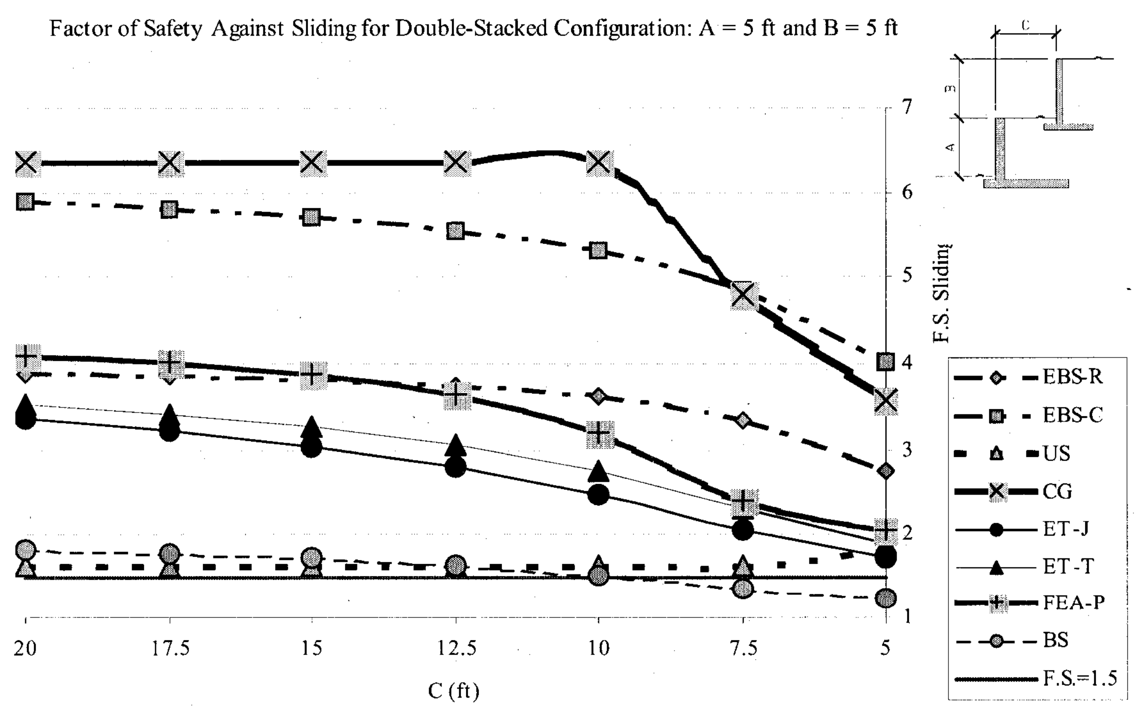

Figure 6.3. Factor of safety against sliding with respect to horizontal offset, C, at double-stacked configuration where height of upper and lower walls, B and A, is 5 feet.

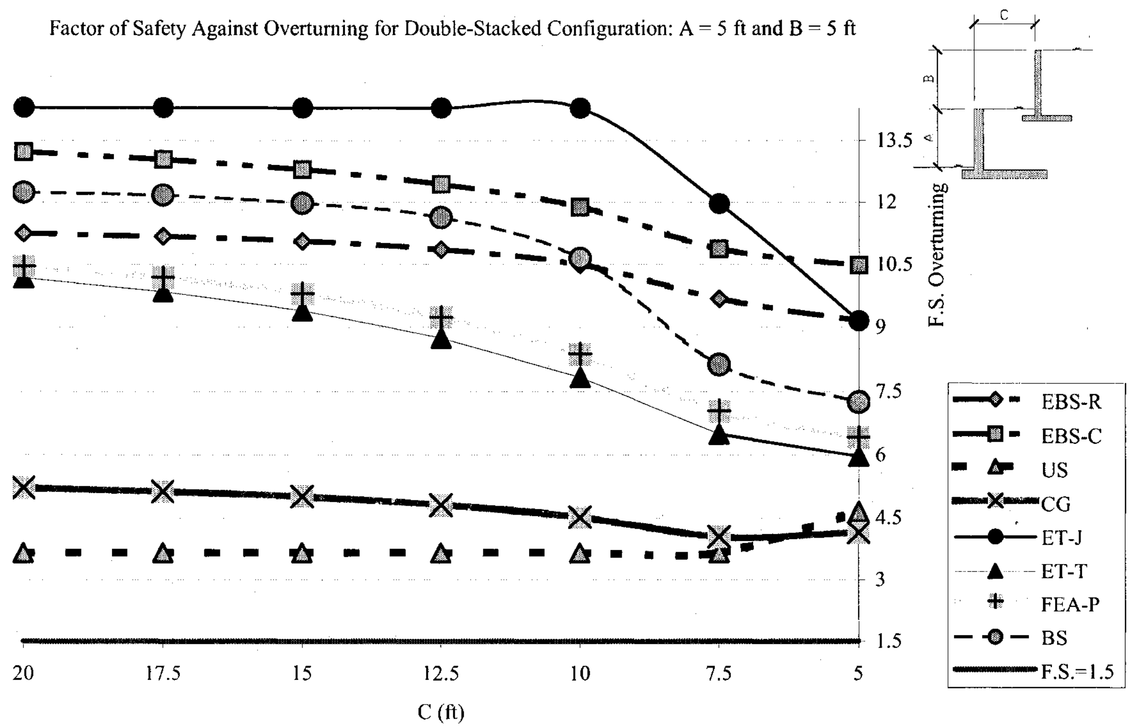

Figure 6.4. Factor of safety against overturning with respect to horizontal offset, C, at double-stacked configuration where height of upper and lower walls, B and A, is 5 feet.

As can be seen in Figures 6.1 and 6.2, the results of analysis with one method may require that the lower wall of the double-stacked configuration be designed for much more sliding or overturning force that a different method may require. Consider the double-stacked configuration 5-15-20. The sliding forces calculated with each method of analysis are presented in Table 6.1. The results presented in this table show that if the Uniform Surcharge (US) method of analysis is selected, the lower wall of the 5-15-20 configuration would be required to be designed for 13.6 times more sliding force than if Culmann's Graphical (CG) method is selected, and 14.9 times as much overturning moment. This is an extreme case, but the average ratio of the maximum to minimum sliding force / overturning moment calculated in the same manner as shown for the 5-15-20 configuration is 3.3 for sliding force and 6.5 for overturning moment. Refer to Table

4.1 for a legend of the marks used to identify the methods of analysis (EBS-R, EBS-C, US, etc.). Tables for all the results for sliding force, overturning moment, factor of safety against sliding, and factor of safety against overturning for all the double-stacked configurations is presented in Appendix F.

Table 6.1. Sliding force and overturning moment at 5-15-20 configuration.

Method of Analysis	Sliding Force	Overturning Moment
EBS-R	0.93 k	2.16 ft-k
EBS-C	0.86 k	2.00 ft-k
US	8.69 k	69.18 ft-k
CG	0.64 k	4.63 ft-k
ET-J	1.32 k	1.49 ft-k
ET-T	1.24 k	2.72 ft-k
FEA-P	0.74 k	2.62 ft-k
BS	2.08 k	1.67 ft-k

At first glance, it may appear that the Uniform Surcharge (US) method is the most conservative, followed closely by Brooks Surcharge (BS) for sliding force, and Culmann's Graphical (CG) for overturning moment. However, this is not the case for all 63 double-stacked configurations. Tables 6.2 through 6.5 present the number of times that a particular method of analysis yields the maximum or minimum value for a given stacked configuration. The tables also present the number of times that the result from a particular method is somewhere in between the maximum and minimum values marked at the mean and median values for each double-stacked configuration (the mean is generally higher than the median).

Table 6.2. Sliding force count. The number of times that a particular method of analysis yields the maximum, minimum, etc., sliding force value for a given stacked configuration

	EBS-R	EBS-C	US	CG	ET-J	ET-T	FEA-P	BS
Equal to the Max.	-	-	24	-	-	-	-	39
Between Max. and the Mean	2	-	24	-	40	5	12	23
Between Mean and the Median	2	-	6	-	23	29	6	1
Between Median and the Min.	43	28	7	28	-	29	38	-
Equal to the Min.	-	19	2	35	-	-	7	-

Table 6.3. Overturning moment count. The number of times that a particular method of analysis yields the maximum, minimum, etc., overturning moment value for a given stacked configuration

	EBS-R	EBS-C	US	CG	ET-J	ET-T	FEA-P	BS
Equal to the Max.	-	-	33	30	-	-	-	-
Between Max. and the Mean	-	-	14	19	1	28	-	14
Between Mean and the Median	16	-	4	14	7	31	7	18
Between Median and the Min.	31	43	8	-	24	4	32	31
Equal to the Min.	-	4	4	-	31	-	24	-

Table 6.4. Factor of safety against sliding count. The number of times that a particular method of analysis yields the maximum, minimum, etc., factor of safety against sliding for a given stacked configuration

	EBS-R	EBS-C	US	CG	ET-J	ET-T	FEA-P	BS
Equal to the Max.	-	19	-	43	-	-	1	-
Between Max. and the Mean	43	28	8	20	-	20	40	-
Between Mean and the Median	-	-	1	-	-	9	4	-
Between Median and the Min.	4	-	30	-	63	34	18	24
Equal to the Min.	-	-	24	-	-	-	-	39

Table 6.5. Factor of safety against overturning. The number of times that a particular method of analysis yields the maximum, minimum, etc., factor of safety against overturning for a given stacked configuration

	EBS-R	EBS-C	US	CG	ET-J	ET-T	FEA-P	BS
Equal to the Max.	-	4	4	-	32	-	23	-
Between Max. and the Mean	31	43	8	-	21	3	33	31
Between Mean and the Median	-	-	-	-	2	1	-	-
Between Median and the Min.	16	-	18	33	8	59	7	32
Equal to the Min.	-	-	33	30	-	-	-	-

Tables 6.2 and 6.3 show that no one particular method of analysis is always the most conservative compared to the other methods of analysis, nor the least conservative. As expected, Tables 6.4 and 6.5 generally follow show the reverse of Tables 6.2 and 6.3. Generally, it appears that the Uniform Surcharge (US) and the Brooks Surcharge (BS) methods yield values on the high end for sliding force, and Uniform Surcharge (US) and the Culmann's Graphical (CG) methods yield values on the high end for overturning moment. However, note also that the Uniform Surcharge (US) method also yields values that are the minimum for sliding force and overturning moment when compared to the other methods. None of the methods yield the highest values for sliding and overturning for 100% of the double-stacked configurations.

The charts shown in Figures 6.5 through 6.8 show all the results for all 63 double-stacked configurations. The charts follow the same format as Figures 6.1 through 6.4, but instead of just plotting the results of the 5-5-5 configuration only, results are plotted for all 63 double-stacked configurations. Starting at the left end of the X axis, the first plot is for 5-5-20, the second for 5-5-17.5, the third for 5-5-15, and so on to 5-5-5. The next plot to the right of 5-5-5 is the plot for 5-10-20, then 5-10-17.5, then 5-10-15, and so on to the plot for 5-10-5. This pattern continues on to the right-most plot, which is 15-15-5.

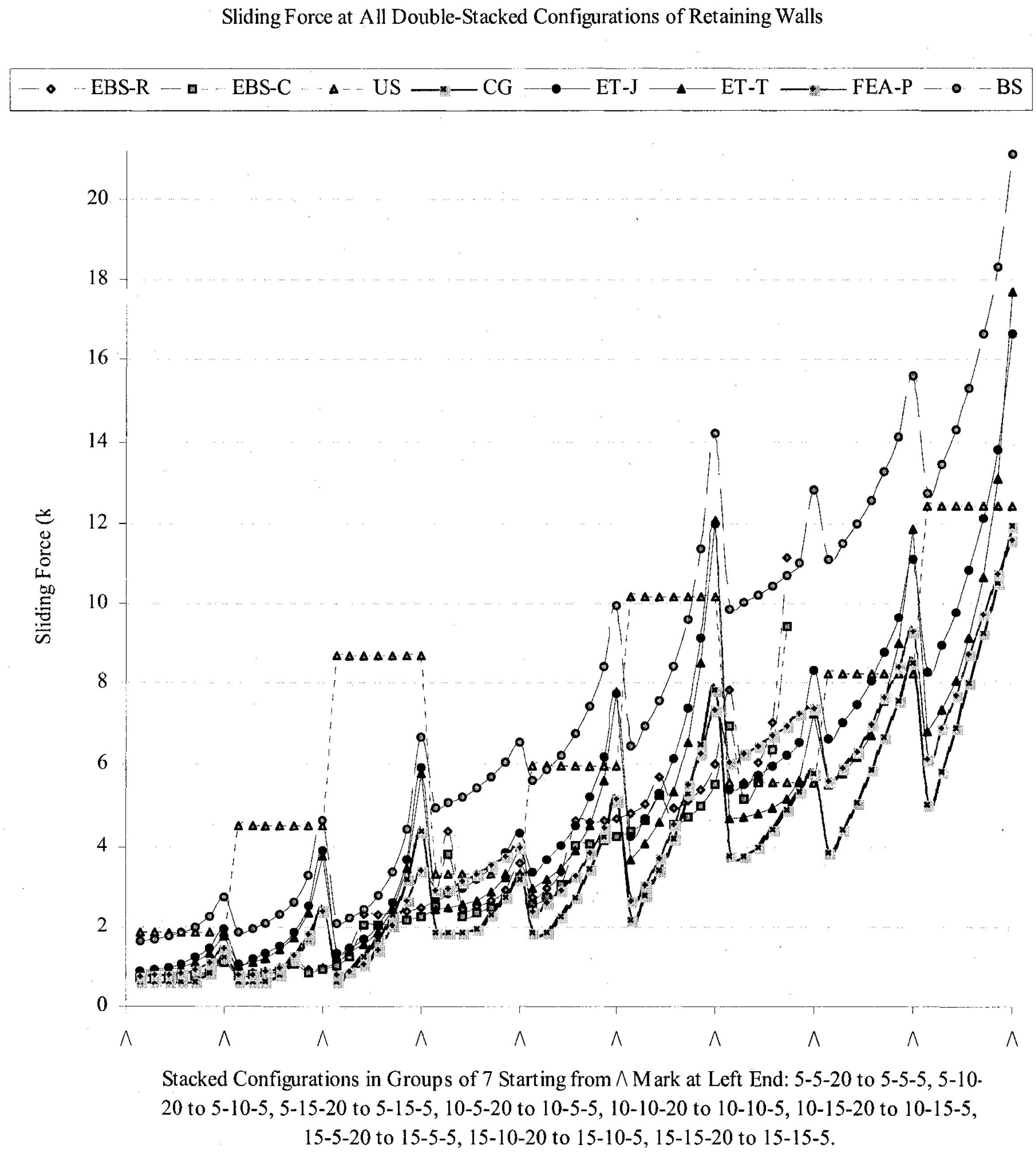

Figure 6.5. Sliding force with respect to horizontal offset, C, at each double-stacked configuration starting at 5-5-20 on the left, and ending at 15-15-5 on the right.

Overturning Moment at All Double-Stacked Configurations of Retaining Walls

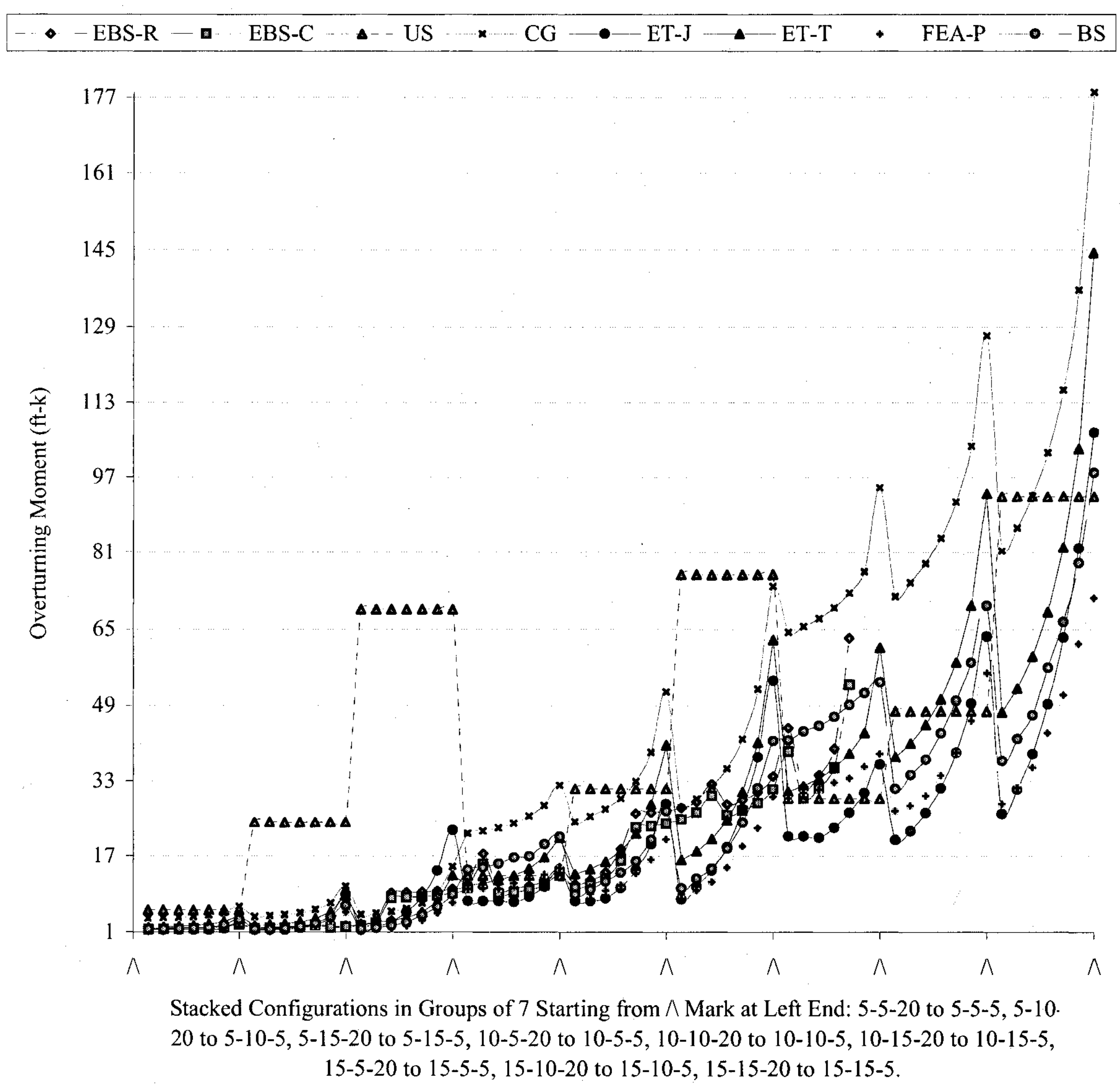

Figure 6.6. Overturning moment with respect to horizontal offset, C, at each double-stacked configuration starting at 5-5-20 on the left, and ending at 15-15-5 on the right.

Factor of Safety Against Sliding at All Double-Stacked Configurations of Retaining Walls

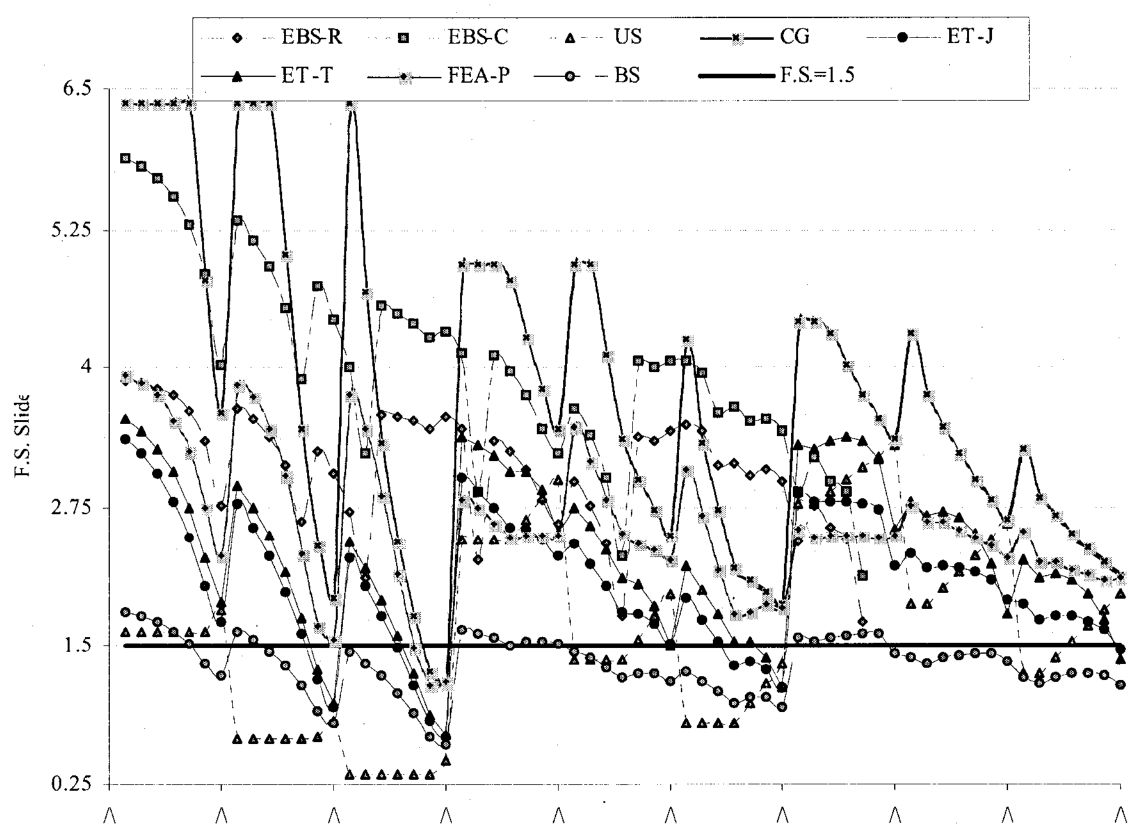

Stacked Configurations in Groups of 7 Starting from /\ Mark at Left End: 5-5-20 to 5-5-5, 5-10-20 to 5-10-5, 5-15-20 to 5-15-5, 10-5-20 to 10-5-5, 10-10-20 to 10-10-5, 10-15-20 to 10-15-5, 15-5-20 to 15-5-5, 15-10-20 to 15-10-5, 15-15-20 to 15-15-5.

Figure 6.7. Factor of safety against sliding with respect to horizontal offset, C, at each double-stacked configuration starting at 5-5-20 on the left, and ending at 15-15-5 on the right.

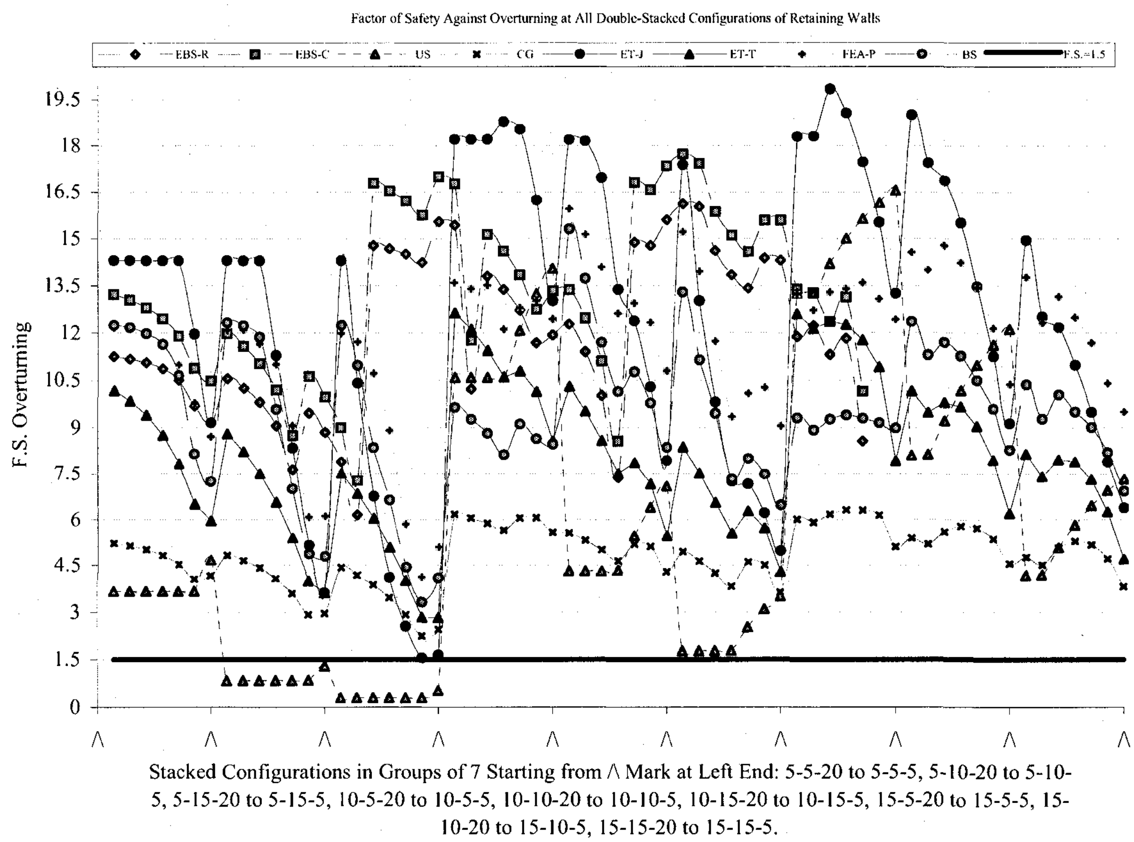

Figure 6.8. Factor of safety against overturning with respect to horizontal offset, C, at each double-stacked configuration starting at 5-5-20 on the left, and ending at 15-15-5 on the right.

Figures 6.5 and 6.6 show that the results for sliding force and overturning moment tend to spread out as the heights of the upper and lower walls (B and A) increase and the horizontal offset (C) between the walls decreases. These figures also give a sense of the magnitude of the difference in results between the more conservative Uniform Surcharge (US) method and the other seven methods of analysis when the height of the upper wall is greater than the height of the lower wall.

Figures 6.7 and 6.8 show that the factors of safety against sliding and overturning tend to converge as the heights of the upper and lower walls (B and A) increase and the horizontal offset (C) between the walls decreases. Perhaps the sliding and overturning forces get smaller when compared to the forces resisting sliding and overturning decreases as the height of the lower and upper walls increase and the horizontal offset decreases.

6.2 Results of Post-Failure Case Study

The eight methods of analysis applied to the 63 double-stacked configurations of retaining walls identified for the thesis study were also applied to the double-stacked configuration of retaining walls that failed in 1992. The resulting sliding force and overturning moments, and factors of safety against sliding and overturning are shown below in Table 6.6.

Table 6.6. Results of analysis of double-stacked failure case study.

Method of Analysis	Sliding Force	Overturning Moment	F.S slide	F.S. overturn
EBS-R *	-	-	-	-
EBS-C *	-	-	-	-
US	12.59 k	73.93 ft-k	0.32	1.49
CG	10.65 k	94.52 ft-k	0.46	1.17
ET-J	10.31 k	66.97 ft-k k	0.40	3.31
ET-T	9.04 k	70.21 ft-	0.45	1.57
FEA-P	9.09 k **	61.70 ft-k	0.45	1.79
BS	13.35 k	38.72 ft-k	0.31	2.85
Olson[3]	15.00 k	75.00 ft-k	0.08	1.13

* Angle of equivalent slope to the horizontal is greater than the soil's internal friction angle, ϕ, Rankine and Coulomb equations for active coefficient do not yield a real number

** Extremely unrealistic deformations are associated with this load

As shown in Figure 6.9 and the results of Olson's analysis presented in his post-failure report[3] and summarized in Table 6.6, the mode of failure for the double-stacked retaining wall appears to be sliding. As shown in Table 6.4, the results of the analysis using the eight methods of analysis are approximately on the same order as the results of Olson's analysis. The sliding forces are lower, but the factors of safety are closely related and predict the mode of failure to be sliding. Similar to the results of the analysis of the 63 stacked configurations, the BS and US methods yield the most conservative results when compared to the results from the other methods.

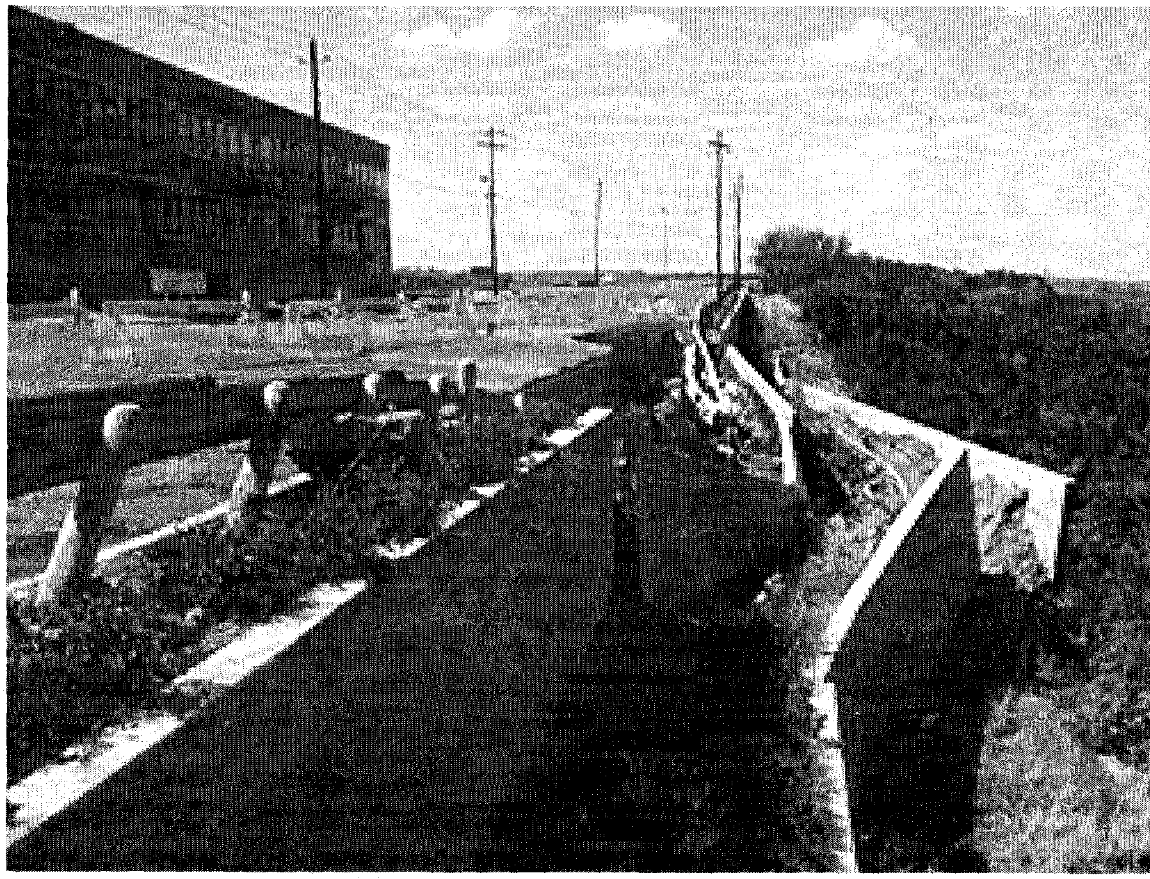

Figure 6.9. Double-stacked retaining wall that failed in 1992 as reported by Olson[3].

CHAPTER 7

CONCLUSIONS AND RECOMMENDATIONS

7.1 Conclusions

This chapter presents conclusions based on the review of the results of each of the 512 analyses. The conclusions are grouped together to provide overall conclusions, and then conclusions regarding each specific method of analysis.

7.1.1 Overall

Generally, the eight methods of analysis used to analyze the 64 different configurations of double-stacked retaining walls predict that as the horizontal spacing, C, between the walls decreases, the sliding force and overturning moments at the lower wall increase. This relationship does not appear to be linear and but rather the resulting sliding forces and overturning moments appear to increase exponentially as the horizontal offset, C, decreases. Retaining wall designers generally agree that these forces increase as C decreases.

The one exception to this general relationship between sliding force / overturning moment and horizontal offset appears to be when the Uniform Surcharge (US) method is used to analyze the double-stacked configurations. The sliding force and overturning moment results from analysis with the Uniform Surcharge method are solely dependent on the height of the upper wall, B, and independent of the horizontal offset, C, and so the sliding force and overturning moment do not change with respect to C.

It appears that as the height of the upper and lower walls in a double-stacked configuration increase, and the horizontal offset decreases, the "spread" between the minimum and maximum values for sliding force and overturning moment appears to increase. This suggests that as the height of the upper and lower walls in a double-stacked configuration increase, and the horizontal offset decreases, the risk of selecting a method which may yield sliding forces and overturning moments that are overly conservative or underly conservative increases. However, the reverse is true for factor of safety: as the height of the upper and lower walls in a double-stacked configuration increase, and the horizontal offset decreases, it appears that the "spread" between the minimum and maximum values for factors of safety against sliding and overturning decreases. There appears to be a "jump" in the factors of safety at values of horizontal offset, C, that correspond to the location of the footing of the upper wall over the footing of the lower wall.

Since the effects of the upper wall were considered to resist overturning and sliding at the lower wall as shown in Figure 3.4, perhaps the largest risk of selecting a method that is overly conservative or underly conservative exists when the footing of the upper wall is close to, but not directly above the footing of the lower wall.

It should be noted that the difference between output for sliding force and overturning moment from each method is potentially very large. In other words, if a retaining wall engineer selects a certain method to analyze a stacked configuration, the engineer may be required to design the lower wall of the stacked configuration for 5 ten or 15 times more force than a different method might require. As such, the retaining wall engineer must take great care in selecting a method of analysis. Further, this underscores the need for research to validate a particular method of analysis or develop an entirely new method.

No one particular method appears to always yield the most conservative results for sliding force and overturning moment. The least conservative scenario appears to be if the Equivalent Backfill Slope method (Coulomb) is used to analyze a stacked configuration for sliding force, while the Elastic Theory (Terzaghi) method is used to analyze for overturning moment. This combination appears to yield the least conservative results.

The methods that appear to yield sliding force results that are on the "high side" are Elastic Theory (Jarquio), Uniform Surcharge, and Brooks Surcharge. The methods, which appear to yield overturning moment results that are on the high side, are Elastic Theory (Terzaghi), Culmann's Graphical, and Uniform Surcharge methods. The scenario which appears to be the best bet to yield the most conservative results is if the Brooks Surcharge method is used to analyze for sliding force, and Culmann's Graphical method is selected to analyze for overturning moment.

7.1.2 Method Specific

The following conclusions are regarding each individual method of analysis. The equivalent backfill slope-based methods of analysis using Rankine and Coulomb theory are grouped together, as well as the elastic theory-based analyses for Jarquio and Terzaghi.

7.1.2.1 Equivalent Backfill Slope

The Equivalent Backfill methods of analysis attempt to take into account the horizontal spacing and geometry of the upper wall. However the use of these methods is limited by the angle of the imaginary line of equivalent slope to the horizontal. When the angle of the equivalent slope is equal to or greater than the angle of internal friction of the backfill material, the equations based on Rankine and Coulomb theory do not yield a real number.

The Equivalent Backfill Slope (EBS-R and EBS-C) methods of analysis yield results for sliding force and overturning moment that appear to follow the other methods of analysis (with the exception of the Uniform Surcharge method) except when the horizontal offset, C, is small. In fact, it appears that the sliding force and overturning moments will "spike" up as C decreases. When the magnitude of C is such that the "spike" in sliding force and overturning moment has not yet occurred, it appears that the values of sliding force and overturning moment are in line with the results of the finite element analysis with Plaxis; just below the median of all the methods. This suggests that the Equivalent Backfill Slope method may be a valid way to estimate the effects of the upper wall at the lower wall of a double-stacked configuration where the horizontal offset is in the range of values greater than the location where the "spike" in sliding force and overturning moment occurs.

Generally, the EBS-R method of analysis appears to yield slightly higher values for sliding force and overturning moment than does the EBS-C method, while the EBS-C method appears to result in higher factors of safety against sliding and overturning that does the EBS-R method of analysis.

7.1.2.2 Uniform Surcharge

The Uniform Surcharge method does not give any consideration to the horizontal offset between the walls, thus yielding the same results for a 5-5-5 double-stacked configuration as for a 5-5-20 configuration. The Uniform Surcharge (US) method of analysis is generally thought to be a conservative approach to analyzing stacked retaining walls when compared to the other methods of analysis. This is true for cases where the height of the upper wall is greater than the height of the lower wall, especially when the height of the upper wall is twice as much or greater than the height of the lower wall. It also appears that the sliding forces and overturning moments resulting from the US method are sometimes the lowest values when compared to the other methods of analysis. This appears to occur when the height of the upper wall is less than the height of the lower wall, and especially when the height of the lower wall is 15 feet.

Because of the tendency for the US method of analysis to result in both relatively high and relatively low values of sliding force and overturning moment, the US method should be used with caution.

7.1.2.3 Culmann's Graphical

Culmann's Graphical (CG) method of analysis appears to closely parallel the results from the finite element analysis with Plaxis (FEA-P). As shown in the charts presented in Figures 6.2 through 6.4, the curve of the CG method and the curve of the FEA-P method appear to have the same slope, and change in slope at approximately the same values of the horizontal offset, C. Method CG tends to yield sliding force values lower than does FEA-P, and overturning values greater than does FEA-P. As the height of the upper wall increases relative to the height of the lower wall, these two methods, CG and FEA-P, appear to yield increasingly closer values for sliding force and overturning moment, especially for the case when the height of the upper wall is three times the height of the lower wall.

The overturning moment resulting from analysis with CG appears to increase as the height of the upper wall increases. Since the location of the resultant sliding force with respect to the bottom of the footing is dependent upon the location of the centroid of the "failure wedge" as shown in Figure 5.9, the tendency for the overturning moment resulting from analysis with CG to increase with the increase in height of the upper wall relative to the lower wall is probably due to a shift outward of the centroid of the "failure wedge."

The CG method of analysis is slightly more complicated than the other methods of analysis that are based on limit equilibrium and appears to do the best job of taking into account the geometry of the stacked configuration and also takes into account ϕ of the backfill soil. The EBS and US limit equilibrium-based methods of analysis attempt to approximate the geometry of the stacked configuration, but have many limitations. The CG method of analysis can be used for any stacked configuration and appears to yield values that are conservative when compared to values resulting from the FEA-P method of analysis, but not overly conservative when compared to the results of the other methods of analysis.

7.1.2.4 Elastic Theory

The methods of analysis based on the elastic theory equations for backfill surface strip load by Jarquio (ET-J) and Terzaghi (ET-T) yields results that are independent of the parameters (ϕ, c, and γ) of the backfill material, but do take into account the geometry of the stacked configuration.

These methods generally yield results that parallel those of the Plaxis finite element (FEA-P) analysis. The ET-J method appears to yield higher sliding forces than does the ET-T method, while the opposite is generally true for the overturning moment. The ET-J and ET-T methods tend to yield values higher that FEA-P for configurations where the height of the upper wall is greater than the height of the lower wall. When the lower wall is 15 feet, the sliding force output for both ET-J and ET-T appear to "spike" as C decreases.

7.1.2.5 Plaxis

The sliding and overturning output from Plaxis (FEA-P) are generally below the median values for all the other methods. The values of sliding force are generally closer to the median values, while the values for overturning moment are generally below the median.

7.1.2.6 Brooks

The results method of analysis proposed by Brooks[2] (BS) appears to follow the results of the other methods which show an exponential increase in sliding force and overturning moment as the horizontal spacing between the walls decreases. Of course, since the BS method is partially based on the ET-J method of analysis, the results of the BS method closely parallel the results of the ET-J method, and are always greater than the values yielded by ET-J. If the results of the US method are neglected, the sliding force results of the BS method are always the maximum value. However, the results for overturning moment are generally below the median as the height of the upper wall increases relative to the height of the lower wall and as the horizontal offset decreases.

7.2 Recommendations

It appears that more research is needed on the topic of analysis of stacked retaining walls. The most critical need is to obtain and analyze experimentally obtained data to validate a particular method of analysis or create an altogether new method of analysis. A study sponsored by the Minnesota Department of Transportation[15] publishes very detailed results of instrumentation of a cantilever concrete retaining wall. The instrumentation included strain gauges on the reinforcing steel, tilt-meters on the footing and wall panels, and earth pressure cells beneath the footing, at the shear key, at the toe of the wall, and at the backfill face of the wall panel. The results of this study are surprising. For example, it is generally thought that the bearing vertical stress distribution at the soil beneath the footing is a highest at the toe of the footing panel, and lower at the rear. The earth pressure cells located beneath the footing measured the opposite condition. Also, it is common practice within the retaining wall design community to use a shear key for sliding resistance, however the earth pressure cells at the shear key did not show that any passive pressure developed at the shear key suggesting that perhaps the shear key may not function as generally thought by the retaining wall design community. Perhaps this study could be used as a model for instrumentation of a stacked configuration of retaining walls.

The charts presented in Appendix G could be used by a retaining wall designer as a decision aid for the selection of a method of analysis to use for a particular configuration. Perhaps a design handbook could be published which shows charts for a larger variety of stacked configurations and soil material properties, providing the retaining wall designer with a more comprehensive aid for selection of a method of analysis. Further, once experimental data is obtained, it could be plotted on a chart similar to the Appendix G charts developed for this thesis and a method of analysis could be selected based on the curve of this experimental data in the chart.

This thesis explores a variety of configurations for a double-stacked condition only. Perhaps similar studies should be done to explore more configurations of stacked retaining walls. Stacked configurations are often constructed with three, four, or even five tiers of retaining walls. Some configurations have sloped backfill between the walls and at the toe of the lowest wall or and backfill of the highest wall. The study presented in this thesis is also limited to cantilever retaining walls. However, gravity retaining walls and mechanically stabilized earth retaining walls are also constructed in stacked configurations and might also be future areas of study.

The system sliding and system overturning analyses presented in this thesis are generally analyzed at the back face of the retaining wall. Some retaining wall designers argue that there are two "planes of analysis" for cantilever retaining walls: one for the analysis for external or system stability and one for internal or flexural stability. The "plane of analysis" for system stability (sliding, overturning bearing) is taken at a vertical plane extending up from the heel edge of the footing, while the "plane of analysis" for the internal stability is taken at a vertical plane extending from the backfill face of the retaining wall. Perhaps this topic could be researched to see if it is makes sense to standardize this practice and/or validate the practice with experimental data.

REFERENCES

1. Jalla, R. (1999). "Design of Multiple Level Retaining Walls." Journal of Architectural Engineering, Volume 5, Number 3, pp. 82-88.
2. Brooks, H. (2006). "Basics of Retaining Wall Design, Sixth Edition." Corona Del Mar, California: HBA Publications, Inc., pp. 47, figure 6-9.
3. Olsen, Roy (1993). "Failure of a Twenty-Foot High Retaining Wall." Proceedings: Third International Conference on Case Histories in Geotechnical Engineering, St. Louis, Missouri, June1 – 4, Paper No. 5.31 .
4. Spangler, M. G., and Mickle, J. (1956). "Lateral Pressure on Retaining Walls Due to Backfill Surface Loads." Highway Research Board Bulletin Number 141, pp. 1-18.
5. Bowles, J. E. (1996). "Foundation Analysis and Design, Fifth Edition." New York: The McGraw-Hill Companies, Inc., pp. 629-634.
6. Boussinesq, J. (1883). "Application des potentials a l'etude de 'equilibre et du movement des solides elastiques." Paris: Gauthier-Villars.
7. Jarquio, R. (1981). "Total Lateral Surcharge Pressure Due to Strip Load." Journal of the Geotechnical Engineering Division, American Society of Civil Engineers, Volume 107, Number GT10, pp 1424-1428.
8. Terzaghi, K. (1954). "Anchored Bulkheads." Transactions, American Society of Civil Engineers, 119: 1234.
9. Spigolon, S. J. (2001), "Geotechnical Engineering." New York: McGraw-Hill, pp. 4.10-4.12, 10.6.

10. Das, B. M. (1999). "Principles of Foundation Engineering, 4th edition." Pacific Grove: PWS Publishing.

11. Das, B. M. (1998). "Principles of Geotechnical Engineering, 4th edition." Boston: PWS Publishing.

12. Culmann, K. (1866). "Die Graphische Statik" (Section 8, "Theorie der Stuta und Futtermauern) Zurich, Meyer und Zeller.

13. Jumkis, A. R. (1962). "Soil Mechanics." Princeton New Jersey: D. Van Nostrand Company, Inc., pp. 559-592.

14. Poncelet, J. V. (1840). "Memiore sur la Stabilite des Revetments et de Leurs Fondation." Note Additionelle sur les Relations Analytiques qui Lient Entre Elles la Poussee et la Butee de la Terre, Memorial de L'Officier de Giene. Paris, vol. 13.

15. Bentler, Labuz, Schultz (2005) "Earth Pressure Behind a Retaining Wall". St Paul, Minnesota: Minnesota Department of Transportation, Report No. 2005-14.

VITA

Graduate College
University of Nevada, Las Vegas

Layne David Weight

Home Address:
10008 Hawthorne Grove Street
Las Vegas, Nevada 89183

Degrees:
Bachelor of Science, Civil Engineering, 2003
Univeristy of Nevada, Las Vegas

Thesis Title:
Analysis of Stacked Retaining Walls

Thesis Examination Committee:
Chairperson, Moses Karakouzian, Ph.D.
Committee Member, Doug Rigby, Ph.D.
Committee Member, Nader Ghafoori, Ph.D.
Committee Member and Graduate College Representative, Brendan O'Toole, Ph.D.